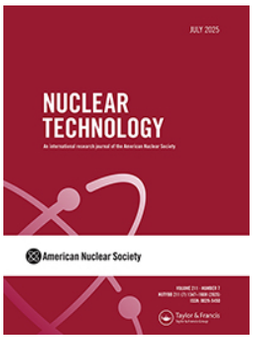

Nuclear Technology

ISSN: 0029-5450 (Print) 1943-7471 (Online) Journal homepage: www.tandfonline.com/journals/unct20

Uncertainty and Sensitivity Analysis for Hot-Leg LOCA in Two-Loop PWR

Andrej Prošek

To cite this article: Andrej Prošek (29 Apr 2025): Uncertainty and Sensitivity Analysis for Hot-Leg LOCA in Two-Loop PWR, Nuclear Technology, DOI: 10.1080/00295450.2025.2463200

To link to this article: https://doi.org/10.1080/00295450.2025.2463200

NUCLEAR TECHNOLOGY

DOI: https://doi.org/10.1080/00295450.2025.2463200

Uncertainty and Sensitivity Analysis for Hot-Leg LOCA in Two-Loop PWR

Andrej Prošek*

Jožef Stefan Institute, Reactor Engineering Division, Ljubljana, Slovenia

Received October 3, 2024
Accepted for Publication January 31, 2025

Abstract — *Overcooling and/or pressurization events have the potential to result in pressurized thermal shock (PTS) in reactor pressure vessels of pressurized water reactors (PWRs). PTS can occur during various overcooling scenarios, including loss-of-coolant accidents (LOCAs). Thermal-hydraulic calculations of overcooling scenarios provide an input to structural analysis. The purpose of this study is to perform advanced thermal-hydraulic calculations of a hot-leg LOCA with uncertainty and sensitivity analyses.*

A novel approach, utilizing a fast Fourier transform–based method (FFTBM) with signal mirroring (SM), is proposed for a sensitivity study to evaluate the influence of input uncertain parameters with low computational cost before performing an uncertainty analysis. For the analysis, a break size of 45.6 cm^2 (equivalent to a 76.2-mm- or 3-in.-equivalent diameter) was selected in a two-loop PWR. A verified and validated RELAP5 input deck was used. In sensitivity study 30, one-at-a-time sensitivity calculations plus reference calculation were performed. These were followed by uncertainty and sensitivity analyses using the GRS (Gesellschaft für Anlagen- und Reaktorsicherheit) Software for Uncertainty and Sensitivity Analyses (SUSA) version 4.2.6 tool, varying 15 uncertain input parameters across 208 samples.

The input uncertain parameters were derived from the European Union–funded Advanced PTS Analysis for LTO (APAL) project. Three figures of merit (FOMs), reactor pressure, liquid temperature, and reactor vessel wall temperature below the cold leg connection, were analyzed. The results demonstrated that FFTBM-SM effectively identified the four most influential parameters, aligning closely with the results from the global sensitivity analysis from SUSA, which utilized 208 samples from the uncertainty analysis.

Although slight differences in parameter ranking were observed, the findings validate FFTBM-SM as a valuable prescreening tool for sensitivity studies. The limitation of the sensitivity study is that it adopts a local approach. Finally, the results of the uncertainty analysis provide tolerance regions for the selected FOMs that are comparable to those obtained in the original APAL study for a four-loop PWR.

Keywords — *Uncertainty analysis, sensitivity analysis, FFTBM-SM, hot leg LOCA, fast Fourier transform–based method with signal mirroring.*

Note — *Some figures may be in color only in the electronic version.*

*E-mail: andrej.prosek@ijs.si

I. INTRODUCTION

The reactor pressure vessel (RPV) of water-cooled reactors of the nonboiling type is one of the most important and nonreplaceable components. Among the risks threatening the integrity of the RPV is possible destruction due to pressurized thermal shock (PTS). PTS can occur during various postulated accident scenarios, such as primary-side pipe breaks

(ranging from small to large break events in terms of probabilistic safety assessments), stuck-open valves on the primary side, main steam line breaks, stuck-open valves on the secondary side, feed and bleed, and SG tube rupture.[1] In the framework of the European Union–funded Advanced PTS Analyses for LTO project (APAL), where LTO stands for long-term operation, a loss-of-coolant accident (LOCA) in the hot leg was selected for analysis in a German-designed 1300-MW four-loop pressurized water reactor (PWR).[2]

In 2021, PTS was studied for a two-loop Westinghouse-type PWR under LOCA scenarios in the cold leg (CL).[3] In the present study, the same two-loop PWR was selected for an uncertainty and sensitivity study of a LOCA in the hot leg. According to the APAL study,[4] a break in the hot leg was considered more conservative for PTS than a break in the CL; therefore, the hot leg break was chosen. The selection of input uncertain parameters was based on results obtained within the APAL project.[2]

A paper from 2023[4] presented how, within the APAL project, the most important thermal-hydraulic phenomena were identified in a phenomena identification and ranking table (PIRT) for a German-designed four-loop PWR with 1300 MW electric power. Once the important thermal-hydraulic phenomena and initial and boundary conditions were identified, the associated parameters in the computer codes were identified. The key identified input uncertain parameters included the capacity of the injection pumps and the temperature of the injected water.

It should also be noted that in the APAL project, the PIRT,[4] which formed the basis for the selection of the input uncertain parameters, was created through expert judgment by project partners. This process incorporated PIRTs developed for other transients, such as those presented in Refs. [1,5]. The PIRT in Ref. [1] was developed for PTS thermal-hydraulic analyses of U.S. PWR plants (the PTS PIRT described in NUREG/CR-6857[6] was revisited and updated based on improved knowledge). The main output parameters of interest when developing PIRTs for PTS included the reactor vessel downcomer pressure, fluid temperature, and wall inside-surface heat transfer coefficient. The PIRT was comprised of 13 phenomena and 10 boundary conditions. The three highest-ranking phenomena were the accumulator (ACC) injection rate, break flow/break size, and reactor vessel wall heat conduction. The highest-ranking boundary conditions were high pressure injection (HPI) flow, ACC injection temperature, and HPI temperature.

The PIRT in Ref. [5] was excerpted from NUREG/CR-6857.[6] The three highest-ranking phenomena identified in the PIRT developed within the APAL project[4] were the safety injection system (SIS) flow rate, ACC injection rate, and liquid/vapor interface in downcomer. The highest-ranking boundary conditions were SIS pumps characteristics, high-pressure safety injection (HPSI) and low-pressure safety injection (LPSI) system temperatures, and secondary depressurization and cooldown timing and rate. A best-estimate plus uncertainty analysis (UA) was also performed to analyze PTS resulting from a LOCA with a break size of 50 cm^2 in the hot leg and loss-of-offsite power for a four-loop PWR coincident with reactor trip, causing reactor coolant pump trip.[7]

The primary aim of this study was to perform UA for an overcooling scenario that had different figures of merit (FOMs) to applications for large-break LOCAs. The pioneering application of UA for a PTS overcooling scenario was conducted within the APAL project.[7] In this study, a different two-loop PWR was considered using the RELAP5 input deck, which has been fully verified and validated.[8] The selected FOMs were based on the APAL proposal and the original study,[1] which was also followed by APAL.

According to Ref. [1], the severity of a transient is controlled by a combination of the initial cooling rate, the minimum temperature during the transient, and the pressure retained in the primary system. For this study, reactor pressure, liquid temperature, and reactor vessel wall temperature below the CL connection were selected as FOMs. The heat transfer coefficient (HTC) was not considered, as it is largely influenced by the input uncertain parameter "single-phase liquid to wall heat transfer coefficient HTC."

The second aim of the study was to demonstrate the importance of performing a sensitivity study before conducting an UA. In the best-estimate methods uncertainty and sensitivity evaluation (BEMUSE) sensitivity analysis, most participants calculate sensitivities using results from the N code runs performed for UA.[9] A paper from 2024[10] stated that sensitivity analysis is an essential part of UA.

Sensitivity analysis is performed both before and after the UA. According to Ref. [10] an a priori sensitivity analysis (i.e., before UA) is necessary for selecting the input and model parameters that contribute most to the uncertainty of safety outputs. An a posteriori sensitivity analysis can then be performed as a byproduct of the UA to compare its results with those of the a priori sensitivity analysis.

A paper from 2025[11] stated that the information obtained through sensitivity analysis using the same set of calculations as for UA can be used, for example, by code developers and experimentalists alike to better focus future resources. The study[12] on the evaluation of functional failure relied on repeated thermal-hydraulic simulations, which are usually time consuming in practice. To address this issue, the RS method was proposed. To use the RS

method, the number of input parameters must be reduced. Consequently, the input uncertain parameters that significantly impact system performance were identified using the Morris method,[12] which helped reduce the dimensionality of the input parameters.

When using the Wilks formula, the number of input uncertain parameters does not affect the number of code runs required. In general, typical applications of thermal-hydraulic system codes do not include a priori sensitivity analysis as proposed in Ref. [10]. That paper[10] stated that, in general, engineering judgment is the most common method used for selecting the input and model parameters that contribute most to output uncertainty. This process was based on the development of PIRTs. No a priori sensitivity analysis was proposed in Ref. [10].

In the original PTS study,[1] sensitivity studies were also employed to guide the uncertainty assessment. Sensitivity evaluation was conducted by varying one parameter at a time, and the results were presented as qualitative statements (e.g., significant effect or insignificant effect).

In this paper, a sensitivity study varying one parameter at a time before the UA is proposed with a quantitative evaluation of the influence of the input parameters. The advantage of this approach is its low computational cost. In this way, the user can obtain quantitative information about the most influential parameters, which were selected through the PIRT process.

It has already been demonstrated that the fast Fourier transform-based method (FFTBM) with signal mirroring (SM) can be used for sensitivity studies.[13] A FFTBM-SM sensitivity study was conducted for the BEMUSE LOFT L2-5 test calculations, which simulated a large-break LOCA. The aim of this study is also to validate the results on the most influential parameters for a hot-leg LOCA obtained in a sensitivity study, with the results obtained from a global sensitivity analysis using the SUSA tool.

The RELAP5 input model and scenario are described in Sec. II. This is followed by a description of the input uncertain parameters and their distributions, the FFTBM-SM methodology, and the uncertainty and sensitivity analysis methods. Section III presents the results for the reference calculation of a hot-leg LOCA and the sensitivity study varying one parameter. It then discusses the UA results obtained from 208 runs, showing the minimum and maximum values of FOMs at each time step representing the lower and upper uncertainty bounds, respectively. Various correlation- and variance-based sensitivity indices for the FOMs are also presented. Section III concludes with a discussion of the results. Finally, conclusions are drawn in Sec. IV.

II. MODELS, SCENARIO, AND METHOD DESCRIPTIONS

First, the RELAP5 input model for the selected two-loop PWR is briefly described. Then the scenario of a hot-leg LOCA with a 45.6-cm^2 (76.2-mm- or 3-in.-equivalent-diameter) break size is outlined. The method descriptions include the selected input uncertain parameters with distributions, FFTBM-SM, the multivariable approach of the Wilks formula obtained by Wald[14] for UA, and the sensitivity indices available in the Software for Uncertainty and Sensitivity Analyses (SUSA) for sensitivity analysis.

II.A. RELAP5 Input Model

For calculations, the RELAP5/MOD3.3lj code developmental version[15] from 2022 was used with several newly built-in uncertainty parameters. Namely, at the request of APAL partners in 2022, RELAP5 was updated to support UAs for PTS. The selected RELAP5 input model of the two-loop PWR has been verified and validated in the past, and has been used in other studies, e.g., Refs. [8,16]. The reactor power was 1994 MW. The input model, shown in Fig. 1, was created using the Symbolic Nuclear Analysis Package (SNAP),[17] and consisted of 304 hydraulic components and 108 heat structures.

The hydraulic components in SNAP include both volumes and junctions, where a pipe with more volumes is counted as one component. All major systems and components were modeled. The input model consisted of the reactor coolant system (RCS) and the secondary system up to the turbine. The RCS included the RPV with the reactor core, two loops, and the pressurizer (PRZ). Each loop consists of hot, intermediate, and CLs, primary-side steam generator (SG) and reactor coolant pump. The break is located in hot leg no. 2, which does not include the PRZ. The secondary side consisted of the secondary-side SGs, main steam lines, main feedwater lines, and the SG relief valves. Among the safety systems, the emergency core cooling system and auxiliary feedwater (AFW) system were modeled. Additionally, the reactor protection and control systems were modeled.

II.B. Hot-Leg LOCA Scenario

The initiating event was a single-side 45.6-cm^2 (76.2-mm- or 3-in.-equivalent-diameter) break in the hot leg, which occurred at 0.01 s, while the reactor was operating at power. This break size is chosen to be like the break size studied in the APAL project. One train of the active emergency core cooling systems was assumed available, including one HPSI pump, one LPSI pump, and both

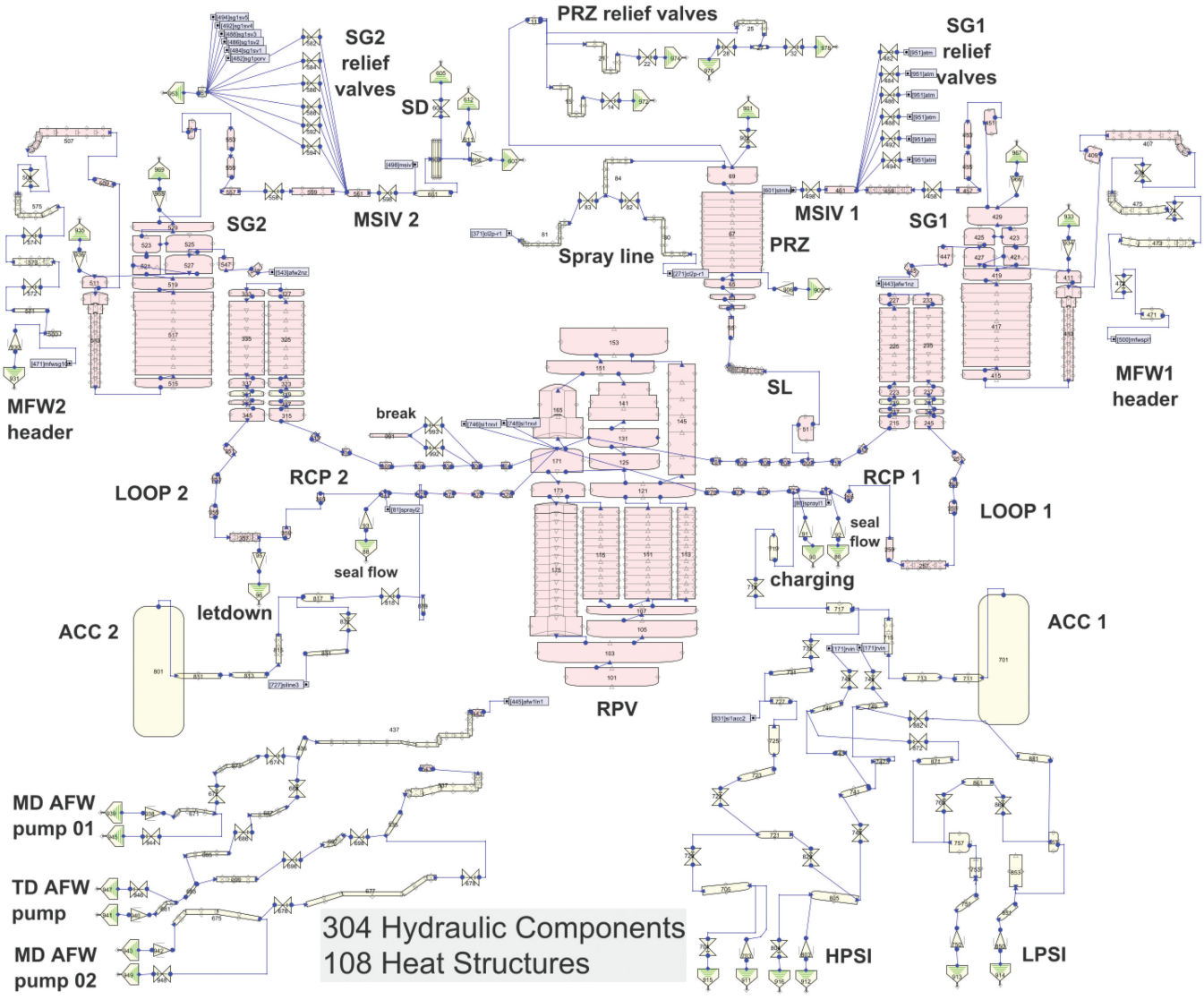

Fig. 1. RELAP5 two-loop PWR hydraulic components view.

ACCs. Both motor-driven (MD) AFW pumps were assumed available.

After the break occurred, the reactor tripped on a low-pressurizer pressure signal (12.99 MPa), which subsequently causes the turbine to trip. A safety injection (SI) signal was generated by the low low-pressurizer pressure signal at 12.27 MPa. Upon the SI signal, active safety systems, including the HPSI pump, LPSI pump, and both MD AFW pumps were activated. The HPSI pump began injection with a 5-s delay following the SI signal. When the primary pressure dropped below 4.96 MPa, both ACCs started injecting. The LPSI pump started injecting when the primary pressure fell below 1.13 MPa. No operator actions were assumed in this scenario.

II.C. Input Uncertain Parameters and Distributions

A total of 15 input uncertain parameters (see Table I) were selected based on results of the APAL project.[1] While APAL considered 19 input uncertain parameters, the following four parameters were excluded in this study due to their small impact in the APAL study: initial secondary-side pressure, ACC nitrogen volume, and the pressure curves for the HPSI and LPSI pumps. The reference (i.e., best estimate) used values shown in column four of Table I.

II.D. FFTBM-SM Method

The original FFTBM,[18] developed by the University of Pisa, quantifies the accuracy of thermal-hydraulic code

calculations against corresponding experimental data. An enhanced version, the FFTBM method with SM, was later developed to address deficiencies in the original approach.-[19] The original FFTBM interprets the time domain signal as an infinite periodic signal. Consequently, the edges of the signal (i.e., differences between the first and the last data points) can significantly contribute to the frequency spectrum amplitudes. This issue can skew the accuracy measure, making it consistent.

The FFTBM-SM eliminates this limitation by symmetrizing the signals through mirroring before applying the fast Fourier transform (FFT), ensuring a more consistent accuracy measure (for details, see Ref. [19]). In the following the FFTBM-SM is briefly described.

The symmetrized reference signal $F_{ref}(t)$ and the difference signal $\Delta F(t)$ are needed to calculate the differences between the two signals. The difference signal in the time domain is defined as $\Delta F(t) = F_{ref}(t) - F_{var}(t)$, where $F_{var}(t)$ is the symmetrized signal with varied input uncertain parameters. The similarity of the signals is based on the amplitudes of the discrete experimental and difference signals obtained by FFT (frequency domain) at frequencies f_k, where $k = 0, 1, \ldots, 2^m$. Here m is the exponent with values $m = 8, 9, 10, 11, 12, 13, 14, 15$. The sampling theorem must be satisfied; therefore, the number of points selection is strictly connected to the sampling frequency.

The FFT algorithm determines the number of points as $K = 2^{m+1}$, which gives a minimum of 512 and a maximum of 65 536 points. Generally, an interpolation is necessary to satisfy this requirement. The FFTBM-SM application implies analysis window T_d selection, the number of points K determination, the cutoff frequency f_{cut} value, and the fixed frequency f_{fix} (minimum maximum frequency of analysis), where T_d, f_{cut}, and f_{fix} are input by user.

A cutoff frequency has been introduced to cut off spurious contributions, generally negligible. The sampling frequency f_s in the FFTBM-SM interpolation algorithm is defined based on the given fixed frequency f_{fix}. To satisfy the sampling theorem, the value of exponent m is determined by the algorithm to ensure that f_{max} is larger than f_{fix}, as follows:

$$f_s = 2f_{max} = {}^{K}/_{T_d} = {}^{2^{m+1}}/_{T_d} \quad . \tag{1}$$

The FFTBM-SM retains the average amplitude from the original FFTBM[18] because all signals are symmetrized before performing FFT. The average amplitude AA_{sm} is calculated as

$$AA_{sm} = \sum_{k=0}^{2^m} |\Delta F(f_k)| \Big/ \sum_{k=0}^{2^m} |F_{ref}(f_k)| \quad , \tag{2}$$

where $|\Delta F(f_k)|$ is the difference signal amplitude at the frequency f_k and $|F_{ref}(f_k)|$ is the reference signal amplitude at the frequency f_k. The AA_{sm} factor is a FOM for similarity of the signals. The greater is the influence of the varied input uncertain parameter on the output signal $F_{var}(t)$, the greater is the difference (discrepancy) between the signals, normally resulting in a greater AA_{sm} value. The FOM is such that it accumulates the discrepancies over time.

The basic idea of FFTBM-SM is to quantify discrepancies using single values, achieved by averaging the amplitude [see Eq. (2)]. The purpose of this quantitative value is not to replace traditional qualitative analysis, including visual observation, but to complement it by providing an additional metric to quantify the compared signals. AA_{sm} represents the relative magnitude of the discrepancy between the variable calculated with one-at-a-time (OAT) input uncertain parameter variation[20] and the corresponding reference variable calculated using the nominal input parameter values. When the variable with OAT input uncertain parameter variation matches the reference variable data, the error function equals zero (with average amplitude also being zero), indicating perfect agreement.

Better accuracy is generally represented by lower AA_{sm} values. A study reviewing quantitative assessments using FFTBM[21] concluded that the FFTBM method effectively ranks generic calculation results. Qualitative evaluation (see Sec. III.B.1) aids in better understanding the results produced by FFTBM-SM and serves as a prerequisite for applying FFTBM-SM in quantitative assessments.

II.E. UA Approach

In UA, input uncertain parameters are propagated through the computer code.[22] Multiple simulations of the transient scenario generate unique data sets, each corresponding to a specific combination of randomly chosen input parameter values. Techniques for uncertainty propagation include Monte Carlo analysis, response surface (RS) methods, and statistical tolerance limits.[23]

Given the computational intensity of the Monte Carlo method for complex thermal-hydraulic codes, statistical tolerance limits based on Wilks' nonparametric methodology are often preferred. In the RS methods, the RS replaces code calculations in the Monte Carlo analysis. Using the statistical tolerance limits approach, input

TABLE I

Input Uncertain Parameters with Distributions

Parameter Number	Parameter Name	Unit	Reference Value/Best Estimate	Distribution Type	Distribution Parameter 1	Distribution Parameter 2	Minimum	Maximum
1	Core power	W	1994.0E6	Normal	1994.0E6	19.94E6	-Infinity (1974.1E6)[a]	Infinity (2013.9E6)[a]
2	PZR pressure	Pa	15.512E6	Normal	15.512E6	0.15512E6	-Infinity (15.357E6)[a]	Infinity (156.671E6)[a]
3	Decay heat	–	1	Uniform	0.9	1.1	0.9	1.1
4	Timing of SIS actuation	s	5	Uniform	0	20	0	20
5	ACC injection temperature	K	322	Uniform	312	332	312	332
6	ACC initial pressure	Pa	4.928E+06	Uniform	4.728E+06	5.128E+06	4.728E+06	5.128E+06
7	HPSI temperature	K	310	Uniform	295	325	295	325
8	HPSI pump flow curve	–	1	Normal	1.0	0.1	-Infinity (0.9)[a]	Infinity (1.1)[a]
9	LPSI pump flow curve	–	1	Normal	1.0	0.1	-infinity (0.9)[a]	infinity (1.1)[a]
10	Initial PZR level	%	55.7	Uniform	48.34	63.06	48.34	63.06
11	Thermal-nonequilibrium coefficient for HF model	–	0.93	Weibull	7	1	0	1.5
12	Single-phase liquid to wall heat transfer coefficient	–	1	Log. uniform	0.8	1.2	0.8	1.2
13	Single-phase vapor to wall heat transfer coefficient	–	1	Log. uniform	0.8	1.2	0.8	1.2
14	Wall-drag coefficient	–	1	Log. uniform	0.5	2	0.5	2
15	Form-loss coefficient	–	1	Log. uniform	0.9	1.1	0.9	1.1

[a]Value used in the sensitivity study.

parameters are randomly sampled N times and the computer code directly generates N outputs, which are then used to estimate the actual uncertainty.

Statistical tolerance limits define the boundaries of an interval for which, with a given confidence level, it can be asserted that the interval contains at least a specified proportion of the population. These limits are derived from a sample and are influenced by the sample size, mean, standard deviation, and the specified proportion within the statistical tolerance limits. As the sample size increases, statistical tolerance limits converge to values determined using population parameters. Moreover, the distribution of the characteristic also affects these limits. For nonnormal characteristics, nonparametric statistical tolerance limits are preferred, as they do not rely on assumptions about the data distribution.

Wilks originally introduced the concept of nonparametric tolerance limits. His study demonstrated that for continuous populations, the distribution of P, the proportion of the population between two order statistics from a random sample, is independent of the population sampled, and it is only a function of the particular order statistics chosen.[23] The Gesellschaft für Anlagen- und Reaktorsicherheit (GRS) was the first one to adopt Wilks' findings for thermal-hydraulic safety analysis, establishing the GRS methodology. This approach can be used to multiple FOMs when they are independent.

The primary advantage of nonparametric statistics is that the number of input uncertain parameters is limited only by user's ability to define and implement uncertainties, and all uncertainties are propagated simultaneously. However, a limitation is that this approach does not produce probability distributions and provides tolerance limits that are conservatively bounding the real limits.

When the number of dependent FOMs is greater than one, the following Wilks formula obtained by Wald (briefly described by Zugazagoitia et al. in Ref. [14]) can be used,

$$\beta = \sum_{j=0}^{N-R^*} \binom{N}{j} \gamma^j \cdot (1-\gamma)^{N-j} \tag{3}$$

$$R^* = p \cdot \sum_{i=1}^{R} d_i \quad , \tag{4}$$

where

N = number of calculation runs

R = number of FOMs

γ = probability content

β = confidence level of the statistical tolerance limits

d_i = number of bounds of the FOMs (upper and/or lower)

p = order.

Examples of the minimum number of samples [i.e., the number of calculation runs N from Eq. (3)] as a function of the number of FOMs for the one- and two-sided tolerance limits, respectively, when the probability $\gamma = 0.95$ and the confidence level β is at least 0.95 (in general, it is slightly higher to satisfy the criterion) are shown in Table II. The number of calculations increases with the number of FOMs. The first step in UA, therefore, is to find the required number of Wilks' samples N for the desired tolerance, confidence level, and number of FOMs using Eq. (3) or Table II.

In this study, three FOMs were used in the UA: (1) primary pressure (FOM1), (2) liquid temperature below the RPV CL inlet (FOM2), and (3) wall temperature below the RPV CL inlet (FOM3). For these three FOMs, the one-sided approach, according to the Wilks formula obtained by Wald, required at least 124 samples, while for the two-sided approach, 208 samples were sufficient to satisfy the criteria that the probability γ was 0.95 and the confidence level β was at least 0.95 (see Table II).

On the other hand, 208 samples were also sufficient samples to consider six FOMs with the one-sided approach. As this analysis was to be input into the fracture mechanics analysis (like the example in Ref. [3]), the input would be 208 calculated trends of three output uncertain parameters calculated by RELAP5, rather than upper and lower uncertainty bounds calculated by the uncertainty methodology. Namely, in the APAL project, it had already been shown that selecting maxima for pressure and minima for temperatures was not useful for fracture mechanics uncertainty quantification. Therefore, the emphasis in this study was to provide 208 runs using randomly sampled input uncertain parameters, and the sensitivity analysis of output uncertain parameters was based on these 208 runs.

II.F. Sensitivity Analysis Techniques

For the sensitivity analysis, the GRS tool SUSA version 4.2.6 was used.[24] Sensitivity analysis helps identify the uncertain input parameters that primarily contribute to the uncertainty of the computational results. For time-dependent sensitivity analysis, SUSA can

TABLE II

Examples of the Minimum Number of Samples for One- and Two-Sided Tolerance Limit, with $\gamma = 0.95$ and $\beta = 0.95$

R	N ($\gamma = 0.95$	Confidence Level β, One Sided	N ($\gamma = 0.95$)	Confidence Level β, Two Sided
1	59	0.951505	93	0.950024
2	93	0.950024	153	0.950555
3	124	0.950470	208	0.950774
4	153	0.950555	260	0.950192
5	181	0.950837	311	0.950350
6	208	0.950775	361	0.950566
7	234	0.950145	410	0.950547
8	260	0.950192	458	0.950154
9	286	0.950715	506	0.950307
10	311	0.950350	554	0.950851
15	434	0.950271	786	0.950408
20	554	0.950851	1013	0.950173
25	671	0.950760	1237	0.950155
30	786	0.950408	1459	0.950328
35	900	0.950289	1679	0.950341
40	1013	0.950173	1897	0.950031
45	1126	0.950610	2115	0.950318
50	1237	0.950155	2331	0.950077
60	1459	0.950328	2762	0.950229
70	1679	0.950341	3190	0.950145
80	1897	0.950031	3616	0.950053
90	2115	0.950318	4041	0.950188
100	2331	0.950077	4464	0.950081

calculate correlation-related sensitivity measures and sensitivity measures derived from correlation ratios (CRs).

The SUSA software implements four correlation based sensitivity indices applicable to individual parameters: Pearson's ordinary correlation, Blomqvist's medial correlation, Kendall's rank correlation, and Spearman's rank correlation. SUSA calculates the ordinary correlation coefficient, the partial correlation coefficient (PCC), the standardized regression coefficient (SRC), and the coefficient of determination (R^2) for each type of correlation. In addition to correlation-related sensitivity measures, the classical CR from original and rank-transformed data can serve as a sensitivity index.

Both the CR from raw data and the correlation ratio from rank (CRR)–transformed data are variance-based sensitivity indices.[24] It is worth noting that the square of the CR is equivalent to the variance-based first-order sensitivity index, also known as Sobol's first-order index. However, Sobol indices in SUSA are calculated only for scalar values, and this option is unavailable for time-dependent sensitivity analysis. The values for CR and CRR range between 0 and 1.

The classical methods for sensitivity analysis are described in detail in Ref. [22]. The following is a brief description of the four correlation-based sensitivity indices. Pearson's correlation coefficient, also known as the ordinary correlation coefficient, describes the relationship between two variables in a bivariate normal distribution. It is commonly used to quantify the dependency between two parameters, X and Y. Blomqvist's medial correlation coefficient, also known as Blomqvist's beta or the population quadrant measure, assesses the degree of association between variables without requiring detailed structural information about their distributions. Analysts can use this measure to incorporate expert judgment on how an increase in parameter X influences parameter Y, relative to the medians m_X and m_Y of their respective distributions.

Kendall's rank correlation coefficient, also known as Kendall's tau, assesses the degree of association between two variables, X and Y. It can be viewed as an extension of Blomqvist's medial correlation coefficient.[22] While both measures have same properties, they differ in their choice of the reference point for concordance. Blomqvist's measure uses a fixed reference point in

terms of the pair of medians (m_X and m_Y), whereas Kendall's measure uses another bivariate parameter pair (X_2, Y_2). Spearman's rank correlation coefficient, also known as Spearman's rho, assesses the degree of association between two random variables, X and Y. It can be considered an extension of Kendall's rank correlation coefficient.[22]

All of these sensitivity indices have values ranging from −1 to 1. Values close to 1 or −1 suggest that the input strongly influences the output, while values close to 0 indicate minimal or no impact. Positive values imply that increasing the input increases the output, while negative values suggest that increasing the input decreases the output. The Pearson sensitivity index is based on linear dependency, and the Spearman and Kendall sensitivity indices are based on monotonic dependency, while Blomqvist's measures the degree of association between two variables relative to their medians (making it useful for nonlinear relationships or scenarios involving outliers). Kendall's rank correlation is generally more conservative than Spearman's rank correlation or Pearson's correlation, meaning its values tend to be slightly lower for the same data. In general, values above 0.7 suggest strong sensitivity.

The (sample) R^2 is provided to evaluate the usefulness of the calculated correlation and regression coefficients as sensitivity indices.[22] R^2 represents the fraction of the variability in the computational result explained by the combined influence of the uncertain input parameters.

The partial correlation measures the degree of association between two variables while controlling for the effect of one or more other variables. It removes the influence of these control variables to focus on the direct relationship between the two variables of interest.

The SRC plays a key role in understanding the relative importance of predictor variables in regression analysis. It quantifies the impact of an independent variable on the dependent variable on a standardized scale (in terms of standard deviations), enabling direct comparison of different predictors' effects on the dependent variable.

Finally, all time-dependent sensitivity index trends are composed of values calculated at the selected time steps. SUSA allows users to select or deselect time values for consideration in time-dependent sensitivity analysis. In this study, the data values used were interpolated, with 501 equidistant values selected for the analysis.

III. RESULTS AND DISCUSSION

In the following subsections, the results of the reference case scenario calculation, sensitivity study, UA, and sensitivity analysis are presented. A discussion of the results is provided at the end.

III.A. Reference Case Scenario

The sequence of events for the reference case scenario was the following. After break occurrence at 0.01 s, the reactor trip signal and turbine trip signals were generated. At 18.89 s, the SI signal was generated. Following a 5-s delay, the HPSI and AFW systems were activated. The ACC began injection at 905 s, and LPSI system started to inject at 2660 s.

For the reference case calculation, the value of the thermal-hydraulic nonequilibrium constant in the Henry-Fauske (HF) choke flow model was not set to a default code value of 0.14. This decision was based on the low likelihood of sampling this parameter value, given its Weibull distribution. Instead, a value of 0.93 was selected, representing approximately the 50th percentile of the Weibull distribution. However, it should be noted that this change in value significantly influenced the results shown in Fig. 2.

Initially, the break flow was higher when the nonequilibrium constant in the HF choke flow model was set to 0.14 (as indicated by the curve labeled SB3HL_HF=0.14 in Fig. 2e). Consequently, the pressure (Fig. 2a) and temperature (see Figs. 2b and 2c, respectively) dropped faster in this case. Due to the faster pressure drop, the HPSI pump, ACCs, and LPSI pump were activated earlier, as shown in Figs. 2f, 2g, and 2h, respectively. Finally, the break mass flow rate and the injection mass flow rates influenced the primary mass inventory, which is depicted in Fig. 2d.

III.B. Sensitivity Study Results

Before conducting the UA, a sensitivity study using OAT variation was performed. It should be noted that sensitivity studies employing OAT variation are not equivalent to sensitivity analysis[20] that require the global variation of input parameters. In the Organization for Economic Co-operation and Development BEMUSE Phase II study,[25] one of the conclusions was that sensitivity calculations using OAT parameter variation should serve as guide for deriving uncertainty bands in subsequent uncertainty and sensitivity analyses.

In this sensitivity study, the minimum and maximum values of uncertain input parameters listed in Table I were used. This approach provided preliminary insights into the impact of the 15 selected input uncertain parameters on the FOMs. However, it is important to note that

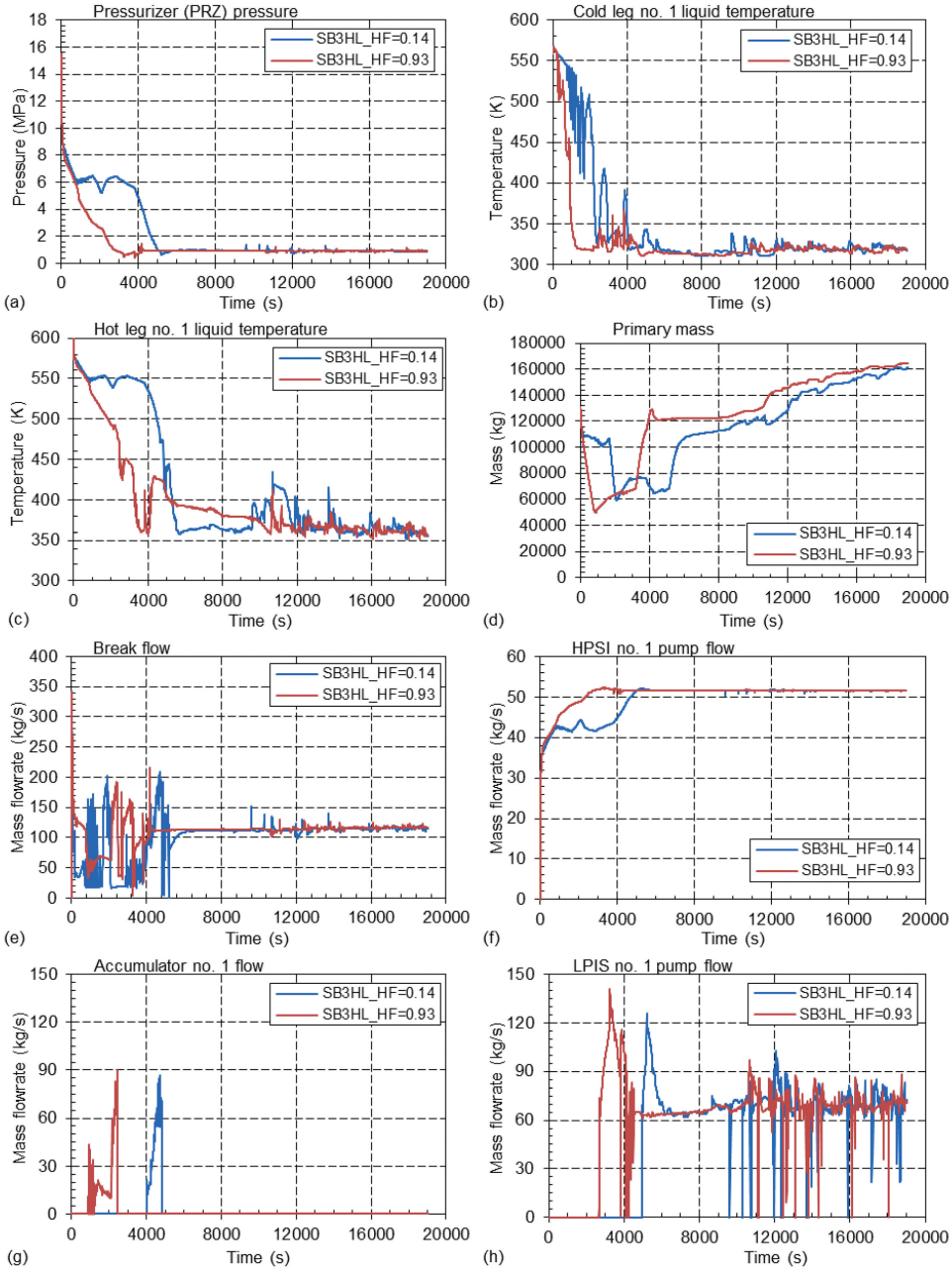

Fig. 2. RELAP5 results for reference case (HF = 0.93) and case with default HF choke flow values (HF = 0.14).

compensating effects between different parameters were not considered in this OAT-based sensitivity study.

III.B.1. Visual Assessment of Input Parameters' Influence

The time trends of the calculated FOMs are shown in Figs. 3, 4, and 5, where the calculated time trends corresponding to the minimum and maximum values of each input uncertain parameter are compared to the reference calculation.

For primary pressure (i.e., FOM1) the time trends shown in Fig. 3 indicate that the most significant discrepancies from the reference trend were caused by Par2_max (initial PRZ pressure) and Par11_min (thermal-nonequilibrium coefficient for the HF choke flow model). Within the 0- to 5000-s time interval, notable discrepancies were also observed for Par3_max (decay heat) and Par15_min (form-loss coefficient). For the remaining OAT parameter variations, the discrepancies from the reference time trend were relatively small, though still visible.

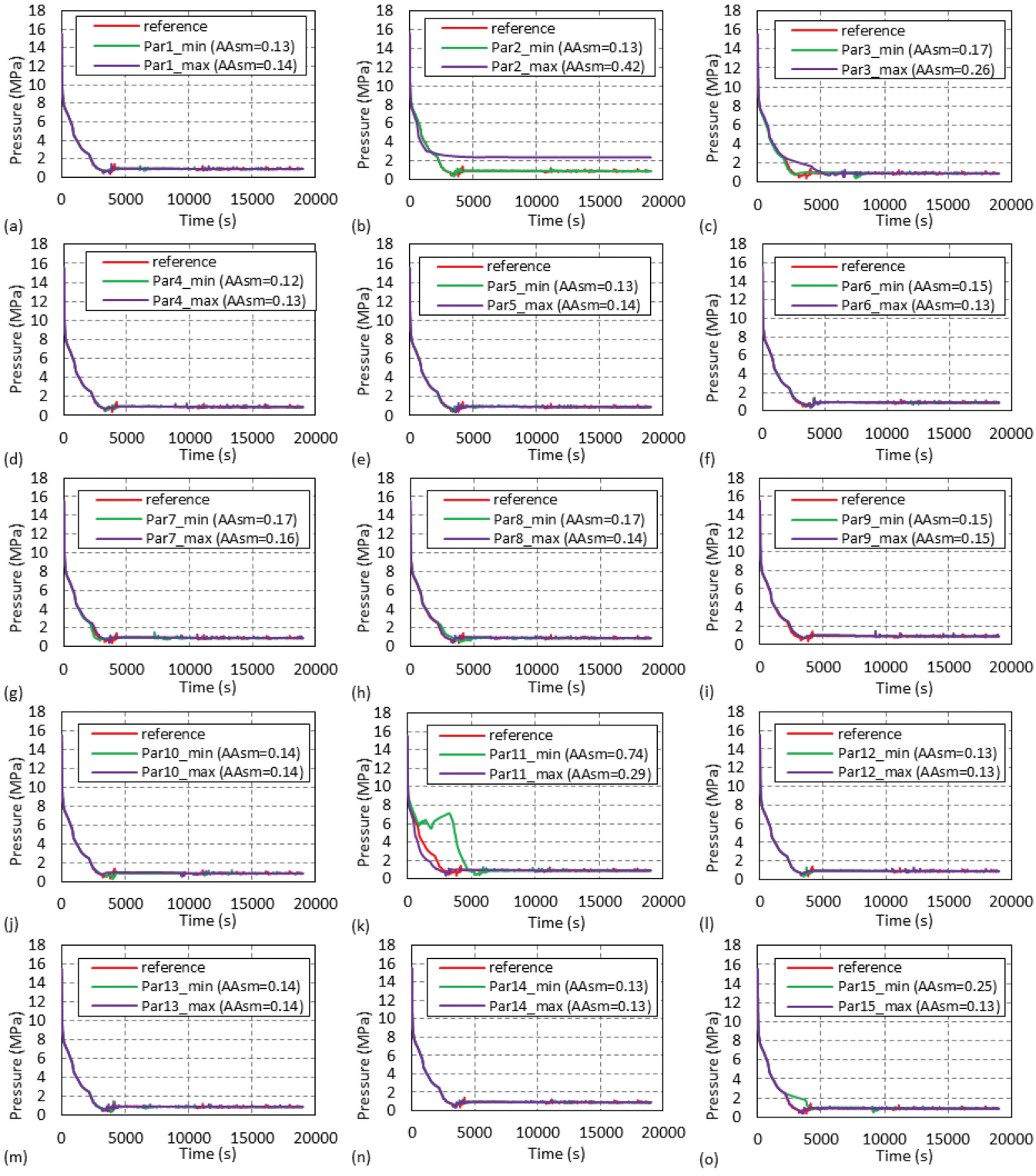

Fig. 3. Primary pressure (FOM1) comparison between reference and OAT parameter variation calculations.

For liquid temperature below the RPV CL inlet (i.e., FOM2), the time trends shown in Fig. 4 revealed that the largest discrepancies from the reference time trend were associated with Par2_max (initial PRZ pressure), Par7_max and Par7_min (HPSI temperature), and Par11_min (thermal-nonequilibrium coefficient for the HF choke flow model). Significant discrepancies were also observed for Par3_max (decay heat) and

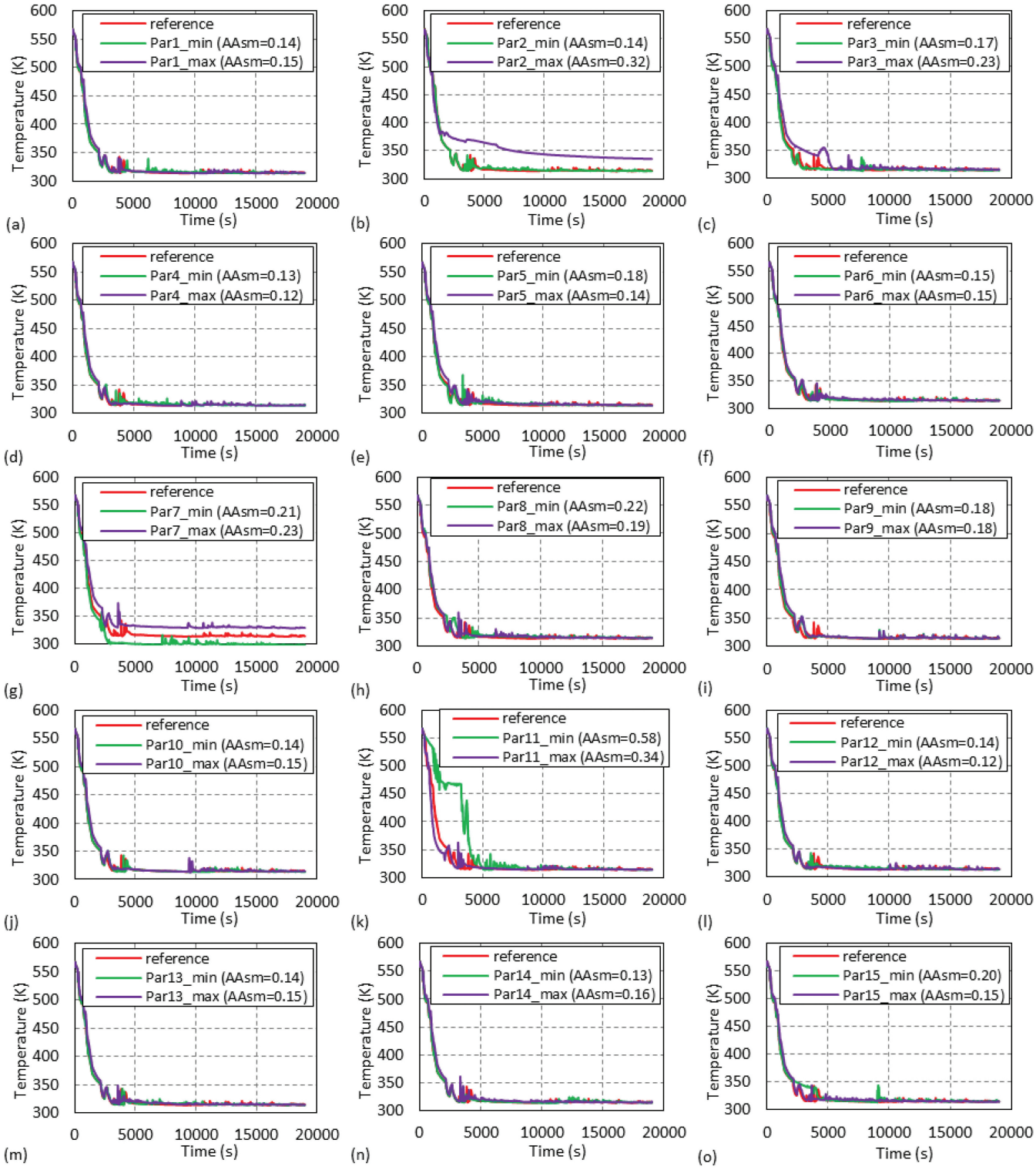

Fig. 4. Liquid temperature below RPV CL inlet (FOM2) comparison between reference and OAT parameter variation calculations.

Par15_max (form-loss coefficient) within the time interval 0 to 5000 s. For other OAT parameter variations, the discrepancies from the reference time trend were relatively small, but remain observable.

The time trends for wall temperature below the RPV CL inlet (i.e., FOM3) are shown in Fig. 5. Visual observation indicated that the largest discrepancies from the reference time trend were caused by Par2_max (initial

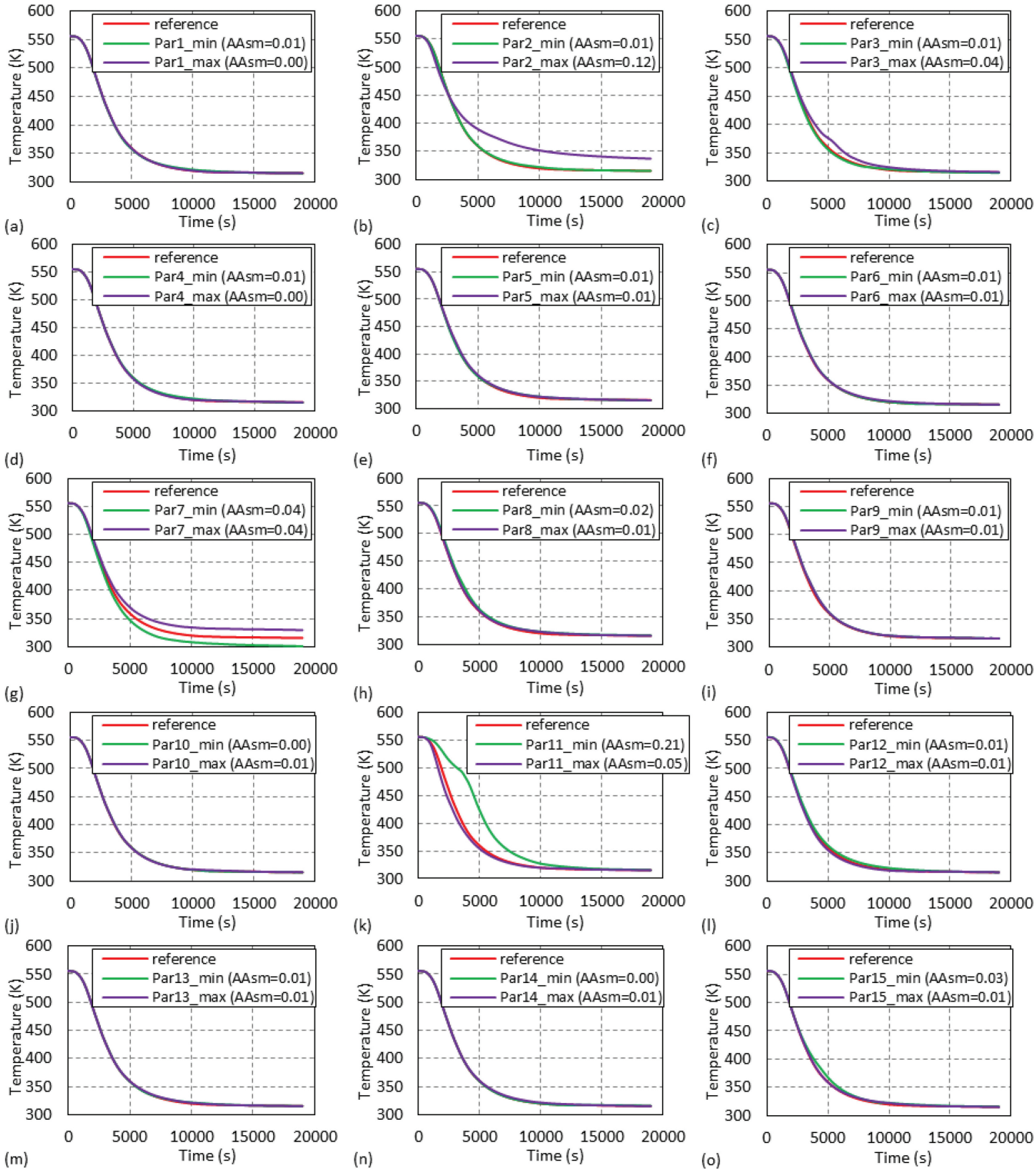

Fig. 5. Wall temperature below RPV CL inlet (FOM3) comparison between reference and OAT parameter variation calculations.

PRZ pressure), Par7_max and Par7_min (HPSI temperature), and Par11_min (thermal-nonequilibrium coefficient for the HF choke flow model). Within the 3000- to 8000-s time interval, a significant discrepancy was also noted for Par3_max (decay heat). For the other OAT parameter variations, the discrepancies from the reference time trend were minimal, with some being nearly imperceptible.

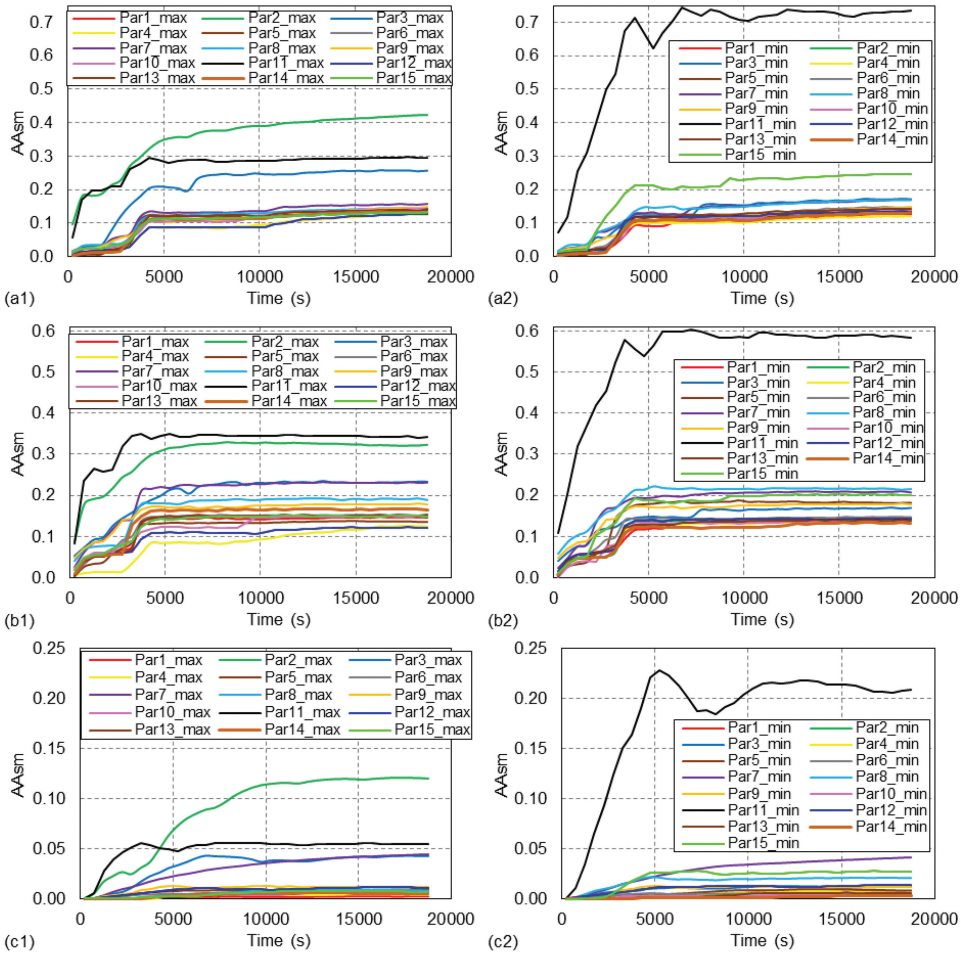

Fig. 6. Average amplitude AA_{sm} for calculations with (left) maximum and (right) minimum input uncertainties: (a) primary pressure, (b) liquid temperature below RPV CL inlet, and (c) wall temperature below RPV CL inlet.

III.B.2. Quantitative Evaluation of Input Parameters' Influence Using FFTBM-SM

The results from the quantitative evaluation of input parameters' influence using FFTBM-SM are shown in Fig. 6, with values of AA_{sm} for time interval 0 to 19 000 s shown in the legend of Figs. 3, 4, and 5. The duration of the signal is an essential factor in comparing two signals by FFTBM-SM, as AA_{sm} is an integral measure.

In this study the transient duration was 19 000 s, and the AA_{sm} shown in Figs. 3, 4, and 5 correspond to this time interval. For the sensitivity study, increasing time intervals were used,[26] starting at time 0 s, with the first time interval being from 0 to 500 s. The subsequent time intervals progressively increased by 500 s, ending at 19 000 s. In total, 38 time intervals were considered. For each of these intervals, the AA_{sm} was calculated, and the time trend of the average amplitude was obtained.

The average amplitude represents the integral sensitivity influence, as it accounts for the history of the parameter variations, thus providing a cumulative assessment. From Fig. 6, the influence of the maximum and minimum values (as seen in the last two columns of Table I) for each of the 15 selected input uncertain parameters on the calculated variables is clearly visible. The calculations for the maximum variations are labeled by Par and the parameter number, followed by _max (e.g., Par1_max for parameter number 1 with the maximum value), while the minimum variations are labeled by Par and parameter number, followed by _min.

The AA_{sm} for primary pressure with maximum input uncertainty variations is shown in Fig. 6a1, and with minimum input uncertainty variations are shown in Fig. 6a2. From these figures, it can be seen that the most sensitive input uncertain parameters for primary pressure were Par2_max (initial PRZ pressure) and Par11_min and Par11_max (thermal-nonequilibrium coefficient for the

HF choke flow model). Other notable sensitive input uncertain parameters included Par3_max (decay heat) and Par15_min (form-loss coefficient). The quantitative sensitivity evaluation by FFTBM-SM aligned very well with the qualitative sensitivity assessment made through visual observations (see Fig. 3).

For liquid temperature below the RPV CL inlet, the AA_{sm} for maximum input uncertainty variations is presented in Fig. 6b1, while for minimum input uncertainty, variations are shown in Fig. 6b2. The most sensitive input uncertain parameters for this FOM were Par11_min and Par11_max (thermal-nonequilibrium coefficient for the HF choke flow model), followed by Par2_max (initial PZR pressure). Other notable sensitive input uncertain parameters included Par3_max (decay heat) and Par7_max (HPSI temperature). Again, the quantitative sensitivity results obtained by FFTBM-SM agreed very well with the qualitative sensitivity findings from the visual observations (see Fig. 4).

For wall temperature below RPV CL inlet, the AA_{sm} for maximum input uncertainty variations is shown in Fig. 6c1, and for minimum input uncertainty, variations are shown in Fig. 6c2. The most sensitive input uncertain parameters for this FOM were Par11_min and Par11_max (thermal-nonequilibrium coefficient for the HF choke flow model), followed by Par2_max (initial PZR pressure). Additional sensitive parameters included Par3_max (decay heat) and Par7_max and Par7_min (HPSI temperature). The quantitative sensitivity judgment from FFTBM-SM aligned very well with the qualitative sensitivity assessment based on visual observations (see Fig. 5).

Overall, the quantitative sensitivity evaluation conducted through FFTBM-SM provided a clear understanding of the influence of the uncertain input parameters on the system's response and complemented the results obtained from visual observations and other sensitivity analysis methods.

III.C. UA Results

All 208 sample runs were completed successfully. The presence of code crashes in the sampling space precludes the application of Wilks' formula. Namely, in most cases the code crashes are functionally related to parameter settings, and therefore the output is no longer independently distributed.[27] The main results of the UA are shown in Figure 7. Figures 7a, 7b, and 7c illustrate the uncertainty of time-dependent results for primary pressure (FOM1), liquid temperature below the RPV CL inlet (FOM2), and wall temperature below the RPV CL inlet (FOM3), respectively. These results are represented by the time histories obtained from the 208 code runs.

Figure 7 also shows the maxima, minima, medians, means, and reference curves obtained from the 208 runs for FOM1, FOM2, and FOM3. For all three FOMs, the reference calculation was bounded by minimum and maximum curves, while there were some differences between the reference and the means curves. Since first order was selected ($p = 1$), the maxima curve represents the time-dependent upper tolerance envelope, while the minima represents the lower time-dependent tolerance envelope, consisting of tolerance limits at selected time steps. When focusing on a scalar value, such as the minimum temperature, this value corresponds to the lowest data point on the minima curve.

III.D. Sensitivity Analysis Results

The time-dependent results for the sensitivity analysis are shown in Figs. 8 through 11. As explained in Sec. II.F, the calculations of sensitivity indices at the selected time steps used 208 code run values corresponding to these steps. Figures 8 and 9 present results obtained using four correlation types: Pearson's ordinary correlation, Spearman's rank correlation, Blomqvist's medial correlation, and Kendall's rank correlation. Figure 10 shows the empirical correlation ratio (ECR) and the CRR. Figure 11 illustrates the PCC and SRC results using these correlation types. Finally, Fig. 12 shows the calculated R^2 for the four correlation types.

Pearson's ordinary and Spearman's rank correlation coefficients for FOM1 indicated that the relationship between input uncertain parameters and output FOMs is strongest for Par11 and Par2 (see Figs. 8a1 and 8a2). This finding aligned with the results of the sensitivity study using visual observation (see Fig. 3) and the quantitative assessment by FFTBM-SM (see Figs. 6a1 and 6a2). The timing of the uncertain input parameters also agreed well. Par2 changed sign while maintaining a significant relationship with FOM1 throughout, whereas Par11 lost significance with FOM1 after 5000 s.

For FOM2 and FOM3, the Pearson's and Spearman's rank correlation coefficients indicated the strongest relationships for Par7, Par2, and Par11 (see Figs. 8b1 and 8b2 for FOM2, and Figs. 8c1 and 8c2 for FOM3). These findings agreed with the sensitivity study results using visual observation (see Fig. 4 for FOM2 and Fig. 5 for FOM3) and the quantitative assessment by FFTBM-SM (see Figs. 6b1 and 6b2 for FOM2, and Figs. 6c1 and 6c2) for FOM3. Parameters Par7, Par2, and Par11 were

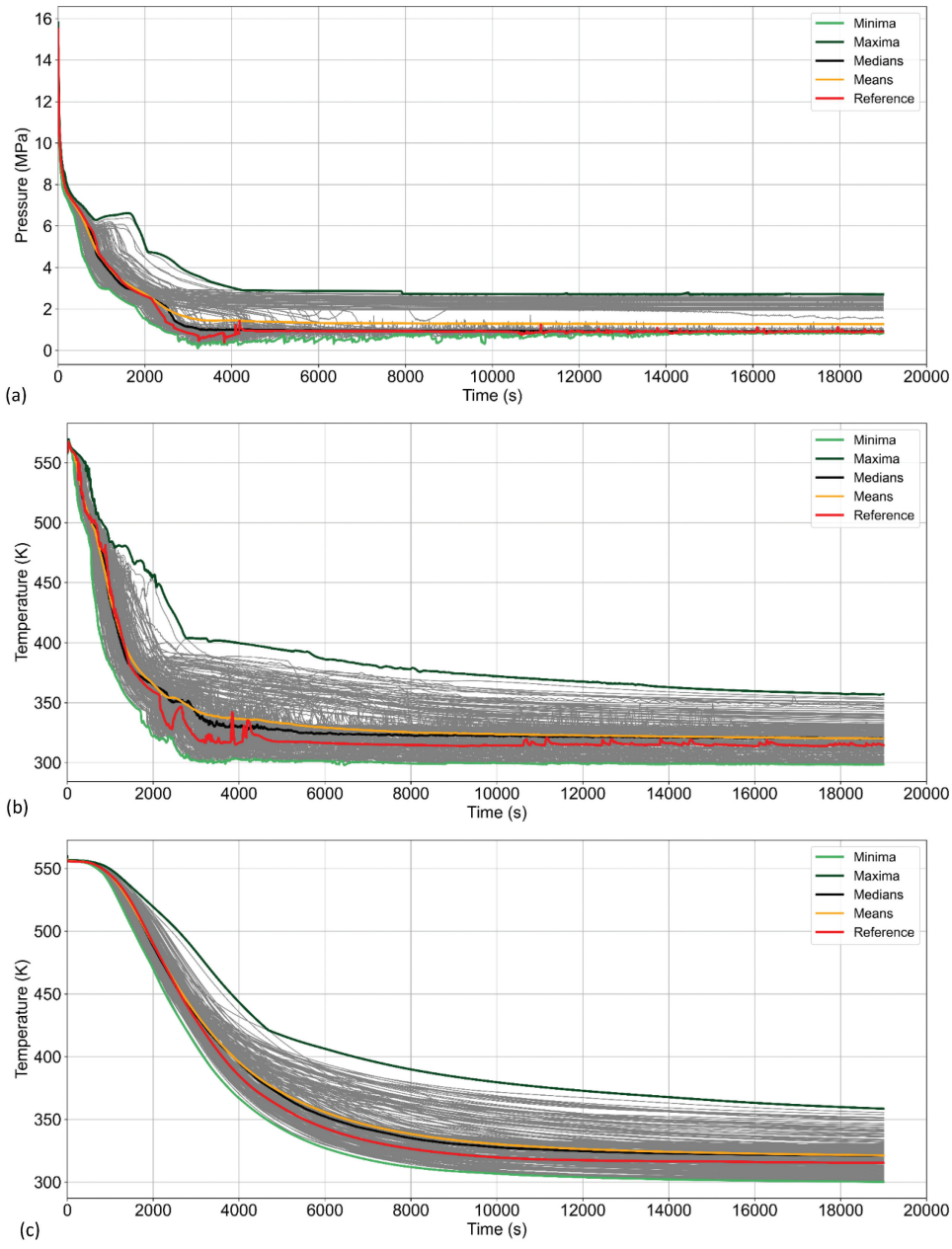

Fig. 7. Total of 208 samples (gray lines) with minima, maxima, medians, means, and reference: (a) FOM1, (b) FOM2, and (c) FOM3.

identified by FFTBM-SM as the fourth, second, and first ranked by influence. The timing also aligned well: Par2 changed sign but maintained significance, Par7 consistently showed a significant positive relationship, and Par11 lost significance with FOM2 and FOM3 after 5000 s.

Blomqvist's medial and Kendall's rank correlation coefficients also indicated strong relationships for FOM1 with Par11 and Par2 (see Figs. 9a1 and 9a2) and particularly large values of sensitivity indices for Par11 of around 2000s. The third largest values of sensitivity index were obtained for Par7 (see Figs. 9a1 and 9a2). This result aligned well with the findings from the sensitivity study using visual observations (see Fig. 3) and the quantitative assessment by FFTBM-SM (see Figs. 6a1 and 6a2).

Blomqvist's medial correlation coefficients and Kendall's rank correlation coefficients showed that the relationship for FOM2 and FOM3 in the first 5000 s was strongest for Par7 (see Figs. 9b1 and 9b2 for FOM2, and Figs. 9c1 and 9c2 for FOM3). For Par11, the sensitivity index values were large, around 2000 s. The third largest

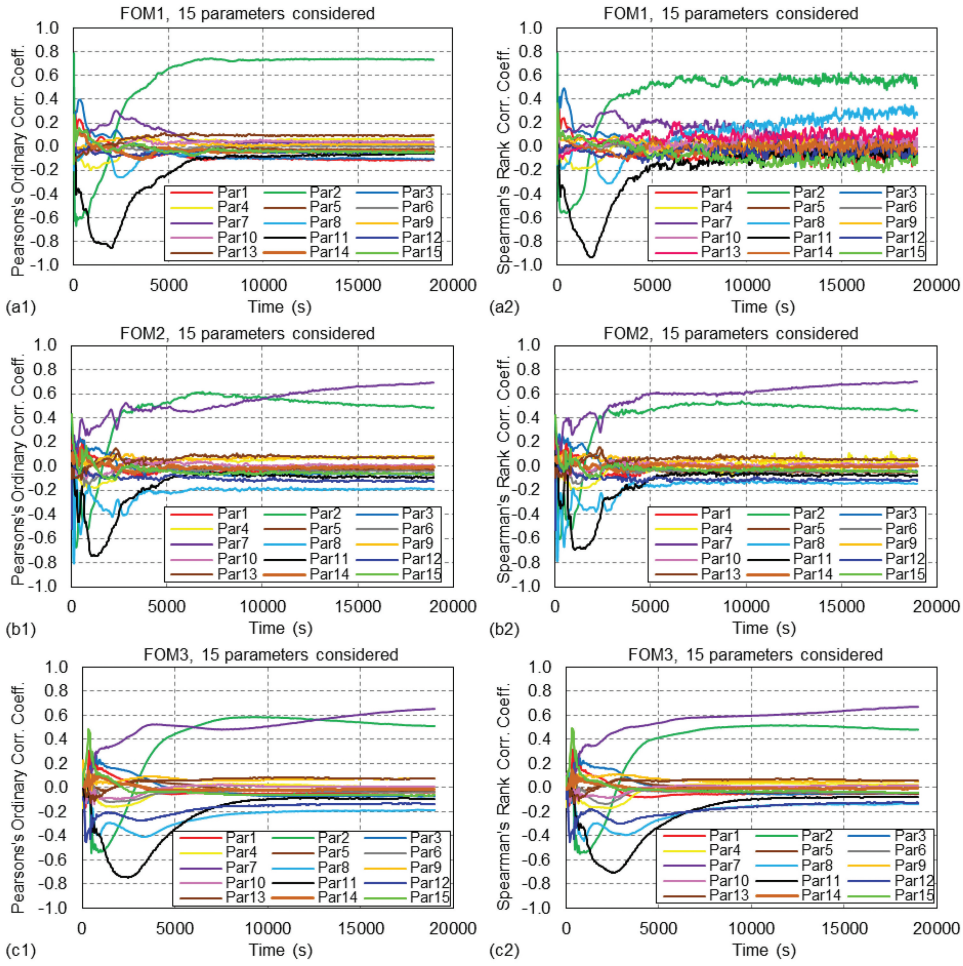

Fig. 8. (left) Pearson's ordinary correlation coefficients and (right) Spearman's rank correlation coefficients for the selected FOMs.

value of the sensitivity index was obtained for Par2. This aligned with the results of the sensitivity study using visual observations (see Fig. 4 for FOM2 and Fig. 5 for FOM3), which identified Par11, Par2, and Par7 as the most influential. Meanwhile, the quantitative assessment by FFTBM-SM (see Figs. 6b1 and 6b2 for FOM2, and Figs. 6c1 and 6c2 for FOM3) identified Par11 and Par2 as the most influential, with Par7 ranked fourth.

The timing for the parameters also agreed well. Par2 and Par7 changed signs and consistently showed a significant relationship with FOM2 and FOM3, except when crossing zero. Meanwhile Par11 after 5000 s had an insignificant relationship with FOM2 and FOM3.

Figure 10 presents the results for the ECR and CRR sensitivity indices. Results for both CRs should be interpreted cautiously due to the low number of code runs, which need to be between 500 and 1000 considering 15 input uncertain parameters. Some of limitations included limited distinction among influential parameters, missed nonlinear influences or interactions between parameters, and the higher likelihood that parameters with high variance in their distributions will appear influential.

The ECRs results indicated parameters Par2 and Par11, and to lesser extent, Par3 and Par8, strongly influenced the variance of FOM1 in the first 5000 s (see Figs. 10a1 and 10a2). This result reasonably aligned with the sensitivity study using qualitative visual observations (see Fig. 3) and quantitative assessment by FFTBM-SM (see Figs. 6a1 and 6a2). The ECR and CRR showed that the strong influence on the variance of FOM2 and FOM3 came from parameters Par11, Par2, and partially Par7. This also agreed reasonably with the results of the sensitivity study using visual observations and quantitative assessment by FFTBM-SM in Sec. III.B. The results suggest that the sensitivity study and sensitivity analysis qualitatively agreed with each other.

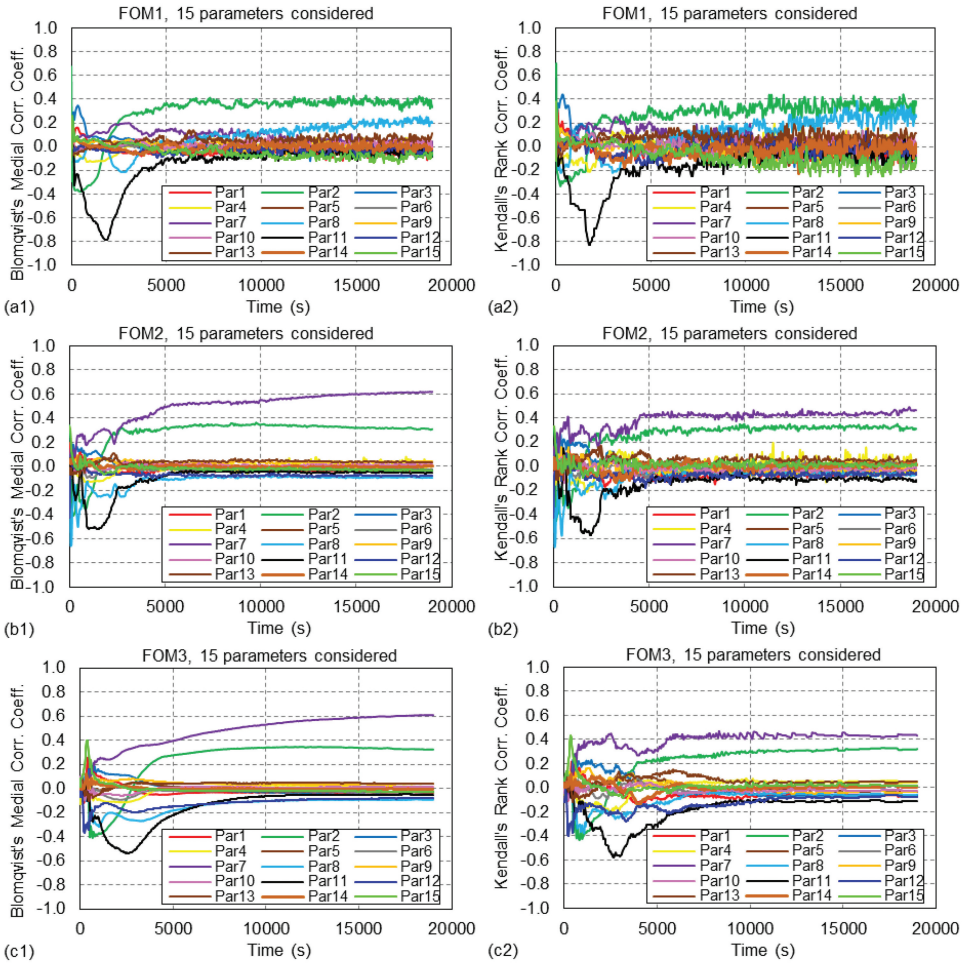

Fig. 9. (left) Blomqvist's medial correlation coefficients and (right) Kendall's rank correlation coefficients for the selected FOMs.

Figure 11 presents the PCC and SRC of the four correlation-based sensitivity indices for the three most significant parameters, as judged by visual observations in Sec. III.B.1. It can be observed that the PCC (left side of Fig. 11) and the SRC (right side of Fig. 11) results are very similar. Additionally, the results obtained using the Pearson's and Spearman's correlation types are close to each other, while the same is true for Blomqvist's and Kendall's sensitivity indices.

Figure 12 presents the R^2 values, which assess the usefulness of the calculated PCC and SRC for the four correlation types for the selected FOMs. For FOM1, the regression model fit the data best with Pearson's correlation, followed by Spearman's rank correlation, while Blomqvist's medial correlation and Kendall's rank correlation produced the worst fits. For FOM2 and FOM3, the regression models fit the data better than in the case of FOM1, with FOM3 fitting slightly better than FOM2. High R^2 values suggest that the independent variable(s) have a strong impact on the outcome (e.g., R^2 values above 0.7 suggest high significance).

Finally, Table III presents the four highest-ranked parameters for each sensitivity index in two time intervals: 0 to 5000 s and 0 to 19 000 s. Since SUSA calculates sensitivity indices at specific time steps, the average values (absolute for the four correlation types) over the time interval were used to rank the input uncertain parameters. On the other hand, FFTBM-SM provides a value for the selected time interval, so the quantitative results were used directly. Having one quantitative value for the entire interval allows for comparison between ranks obtained by SUSA and FFTBM-SM. The time interval 0 to 5000 s was selected because major discrepancies in the FOM2 and FOM3 trends occurred before 5000 s (see Figs. 4 and 5). The second time interval corresponded to the transient duration.

The results for the time interval 0 to 5000 s showed that the majority of sensitivity indices identifies the

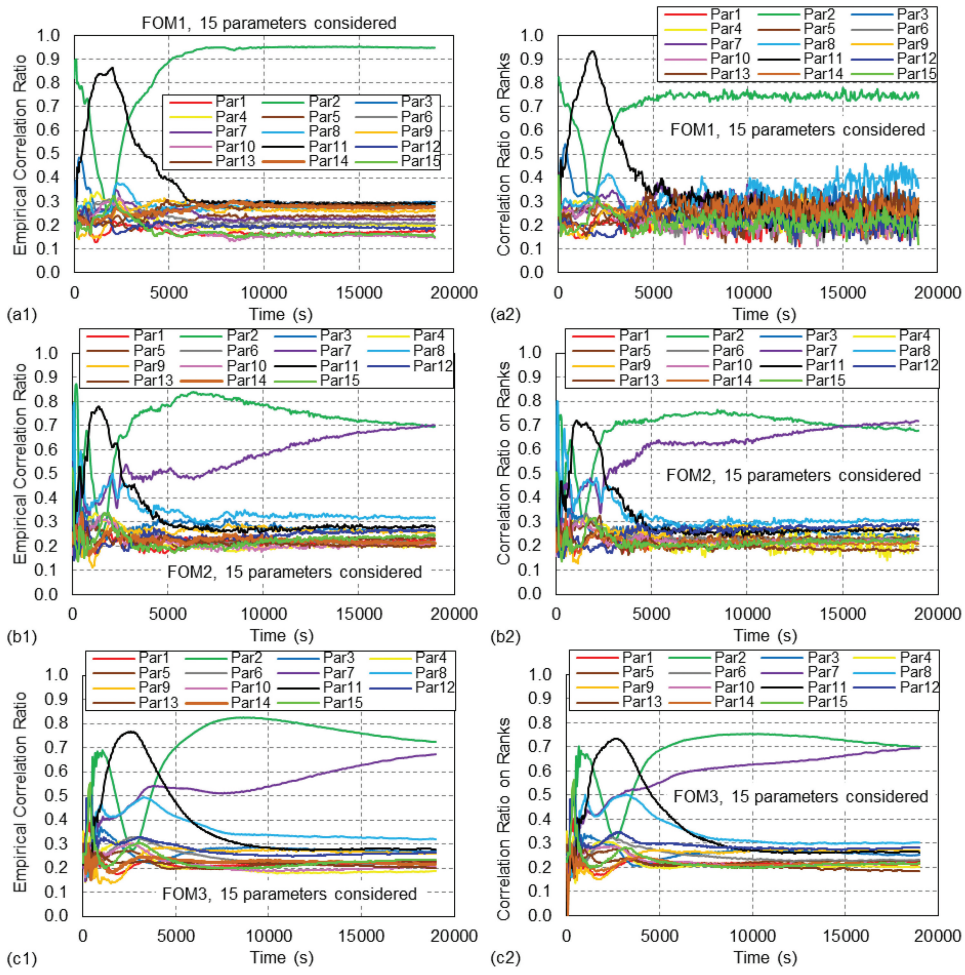

Fig. 10. (left) ECR and (right) CRR for the selected FOMs.

following four input uncertain parameters as influential: thermal-nonequilibrium coefficient for the HF model (number 11), PZR pressure (number 2), HPSI temperature (number 7), and decay heat (number 3) for FOM1; for FOM2, HPSI temperature (number 7), PZR pressure (number 2), thermal-nonequilibrium coefficient for the HF model (number 11), and HPSI pump flow (number 8); and for FOM3, thermal-nonequilibrium coefficient for the HF model (number 11), HPSI temperature (number 7), HPSI pump flow (number 8), and PZR pressure (number 2). In only a few cases, specifically with ECR, CRR, and FFTBM-SM, one parameter out of four differed from this list.

These results show that a limited sample size leads to inconsistencies between the classical CR calculated from the original and rank-transformed data, which affected the ranking in two out of six cases. Specifically, for FOM1 in the time interval 0 to 19 000 s, parameters 3 and 8 reversed their rankings for positions 3 and 4. Similarly, for FOM2 in the time interval 0 to 5000 s, parameters 11 and 7 reversed their rankings for positions 2 and 3.

The results for the time interval 0 to 19 000 s showed that PZR pressure (number 2) and the thermal-nonequilibrium coefficient for the HF model (number 11) were always among the four most influential input uncertain parameters for all FOMs, while HPSI temperature (number 7) was always among the four most influential input uncertain parameters for FOM2 and FOM3.

III.E. Discussion of Results

The main advantage of the GRS methodology using the Wilks findings is that the number of necessary calculations N for a given γ/β tolerance limit is independent of the number of uncertain input parameters. The paper in Ref. [11] states that this independence eliminated the need for a priori ranking and the preselection of input uncertain parameters. However, this can only hold true if the exhaustive list of input uncertain parameters and their

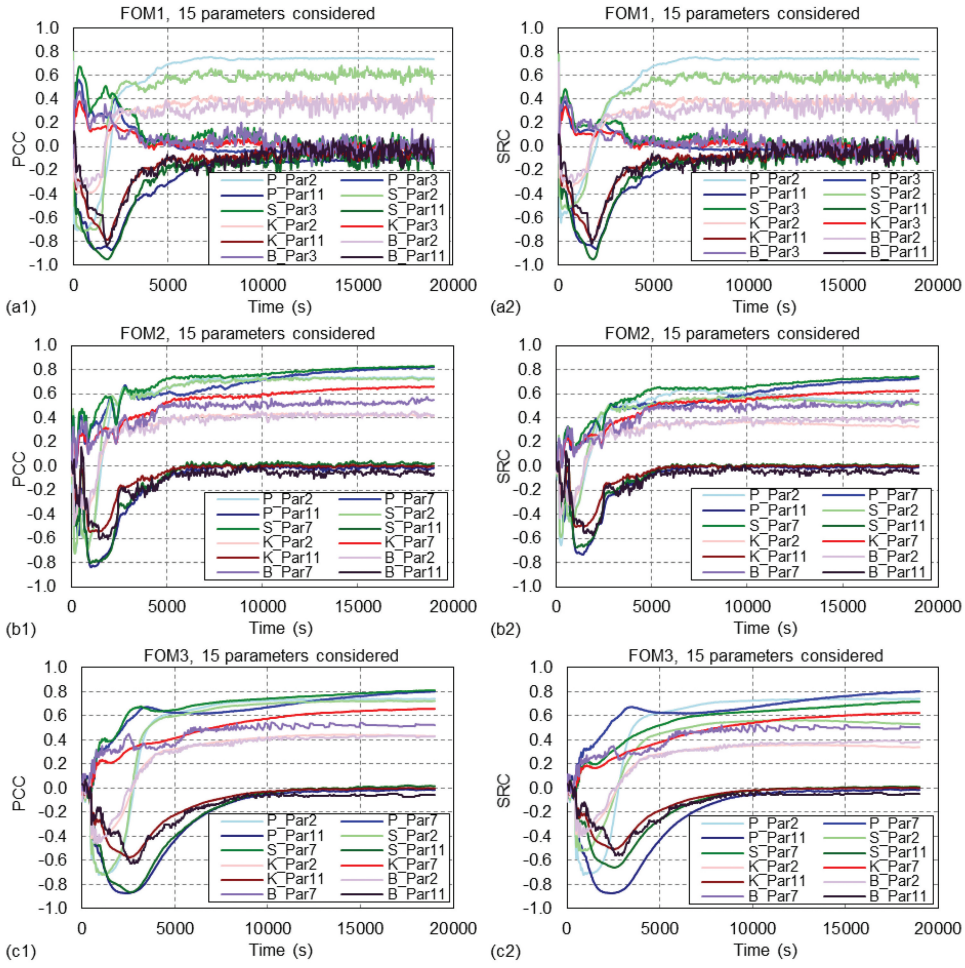

Fig. 11. PCCs and SRCs of the three most significant parameters obtained by the four correlation types for the selected FOMs.

distributions, covering phenomena and boundary and initial conditions, is provided by the code developer.

When using other approaches, which rely on PIRT, the screening of phenomena and the processes are done with the purpose of reducing the extremely large number of modeling parameters in the code to a much smaller number, the uncertainties of which can significantly affect uncertainty of predicting FOMs.[28] The highest-ranked phenomena, and initial and boundary conditions in the APAL PIRT analysis-[4] were SIS flow rate, SIS pump characteristics, and HPSI and LPSI temperatures.

III.E.1 Sensitivity Study versus PIRT

In this study, PIRT was not performed, with the sensitivity study done instead. The results of the sensitivity study showed how much the input uncertain parameters, the selection of which was based on the APAL PIRT, were influential. These results may then be used as guidance for deriving the uncertainty bands. By using such an approach, the input uncertain parameters were also treated from a physics perspective, rather than only statistically after the UA was completed. The input uncertain parameters were HPSI temperature (number 7), HPSI pump flow (number 8), and LPSI pump flow curve (number 9).

The HPSI and LPSI flow rates further depend on the RCS pressure (number 2), which is a global state parameter. A rather important boundary condition was also decay heat, represented by the parameter decay heat (number 3). High HPSI and LPSI flow rates with the low injection flow temperatures most overcool the RPV. On the other hand, the ACC initial pressure and temperature, the timing of SIS injection, and the break flow rate were ranked as medium important, represented by input uncertain parameters numbers 6, 5, 4, and 11, respectively.

Plant initial state (power and PZR pressure) was considered less than medium important (represented by input uncertain parameters numbers 1 and 2, respectively). As the influence of the input uncertain parameters

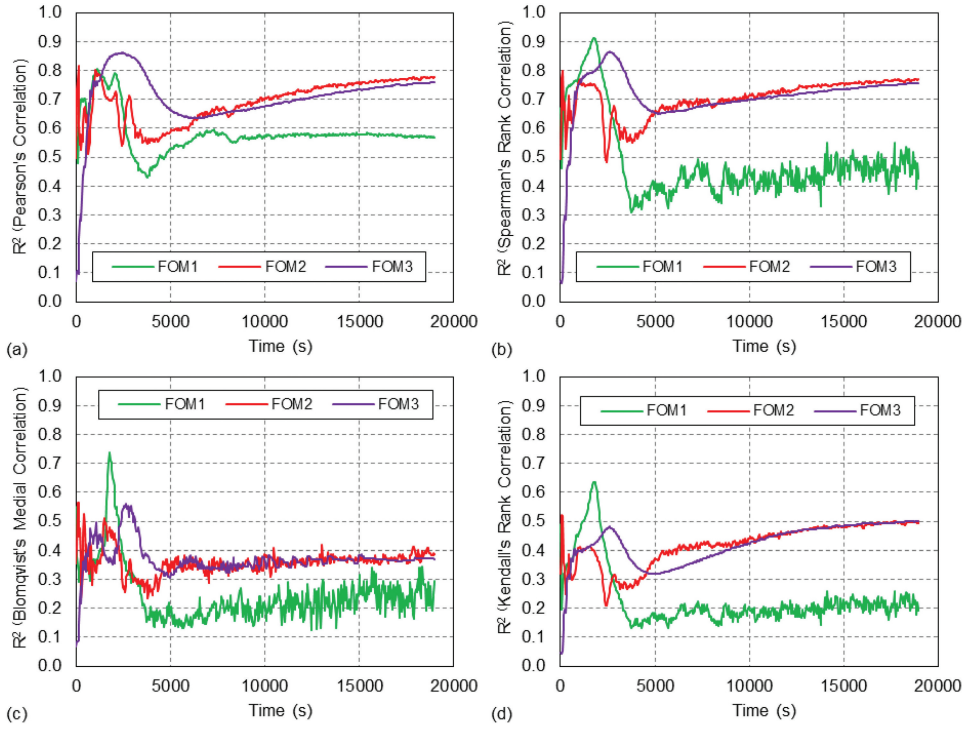

Fig. 12. R^2 for the four correlation-based indices of the selected FOMs.

depends on the uncertainties themselves or on the strength of impact, or both, a sensitivity study was performed before starting UA to get preliminary information on how influential the input uncertain parameters are.

III.E.2 Sensitivity Study Results in Support to Uncertainty Analysis

The results of the sensitivity study suggest that for primary pressure (FOM1), the most influential parameters were parameter 11 (choke flow coefficient), representing break flow phenomenon; parameter 2 (PZR pressure), representing plant initial state; parameter 3 (decay heat), representing decay heat phenomenon; and parameter 15 (form-loss coefficient), representing break flow phenomenon. As primary pressure depends on the break flow, the initial value of primary (PZR) pressure and decay heat influenced the primary pressure (by driving steam generation, affecting the rate of depressurization and interacting with emergency cooling measures). The form-loss coefficient influenced the break flow. From a physics perspective, the selected most influential input uncertain parameters were reasonably justified.

For liquid temperature below RPV CL (FOM2), the sensitivity study also suggested that parameters 11, 2, and 3, as for FOM1, plus 7 and 8 (HPSI temperature and HPSI pump flow curve) were influential ones. Break flow was the most important factor in determining the RCS cooldown and depressurization rate. It directly impacted the ACC and SIS injection flow. Decay heat load directly affected the downcomer conditions, influencing how much steam was generated. Cold water initially tended to lower the pressure by cooling the primary system, but subsequent steam generation due to reboiling may cause temporary increases in pressure.

The HPSI temperature affected the downcomer water temperature, while the HPSI flow rate directly affected the downcomer conditions, principally temperature. The sensitivity study results showed that in the first part of the transient until 5000 s, the HPSI temperature was more influential, and that later when the pressure stabilized, the HPSI pump flow was more influential. Early on, the HPSI temperature is crucial for thermal management and pressure dynamics in a high-energy system. It directly affects the downcomer temperature. Later in the transient, the HPSI pump flow becomes critical for ensuring sustained core cooling and system stabilization as the system transitions to a steady-state condition.

For wall temperature below RPV CL inlet (FOM3), the sensitivity study suggested parameters 11, 2, 3, and 7 as influential ones. Localized wall temperatures were more sensitive to the temperature of the injected coolant (parameter 7) and its mixing characteristics, which overshadowed the influence of the flow rate (parameter 8). It

TABLE III

Four Highest-Ranked Parameters as Quantified by Sensitivity Indices in the Time Intervals 0 to 5000 s and 0 to 19 000 s

Correlation Type/Method	Parameter Numbers for Ordinary (0 to 5000 s/0 to 19 000 s)	Parameter Numbers for PCC (0 to 5000 s/0 to 19 000 s)	Parameter Numbers for SRC (0 to 5000 s/0 to 19 000 s)
	FOM1: Primary Pressure		
Pearson's	11, 2, 7, 3/2, 11, 1, 3	11, 2, 3, 7/2, 11, 7, 13	11, 2, 3, 7/2, 11, 7, 13
Blomqvist's	11, 2, 7, 3/2, 11, 8, 15	11, 2, 3, 7/2, 8, 11, 7	11, 2, 3, 7/2, 8, 11, 7
Kendall's	11, 2, 7, 3/2, 11, 8, 7	11, 2, 3, 7/2, 11, 8, 7	11, 2, 3, 7/2, 11, 8, 7
Spearman's	11, 2, 7, 3/2, 11, 8, 7	11, 2, 3, 7/2, 8, 11, 7	11, 2, 3, 7/2, 11, 8, 7
ECR	2, 11, 8, 3/2, 11, 3, 8	–	–
CRR	2, 11, 8, 3/2, 11, 8, 3	–	–
FFTBM-SM	11, 2, 3, 15/11, 2, 3, 15	–	–
	FOM2: Liquid Temperature Below the RPV CL		
Pearson's	7, 2, 11, 8/7, 2, 8, 11	2, 7, 11, 8/2, 7, 8, 11	2, 7, 11, 8/7, 2, 8, 11
Blomqvist's	7, 11, 2, 8/7, 2, 11, 8	7, 11, 2, 8/7, 2, 4, 11	7, 11, 2, 8/7, 2, 4, 11
Kendall's	7, 2, 11, 8/7, 2, 8, 11	7, 2, 11, 8/7, 2, 8, 11	7, 2, 11, 8/7, 2, 8, 11
Spearman's	7, 2, 11, 8/7, 2, 8, 11	2, 7, 11, 8/7, 2, 8, 11	7, 2, 11, 8/7, 2, 8, 11
ECR	2, 11, 7, 8/2, 7, 8, 11	–	–
CRR	2, 7, 11, 8/2, 7, 8, 11	–	–
FFTBM-SM	11, 2, 3, 8/11, 2, 7, 3	–	–
	FOM3: Wall Temperature Below the RPV CL Inlet		
Pearson's	11, 7, 8, 2/7, 2, 8, 11	11, 8, 2, 7/2, 7, 8, 11	11, 8, 2, 7/2, 7, 8, 11
Blomqvist's	11, 7, 8, 12/7, 2, 11, 12	11, 7, 2, 8/7, 2, 11, 4	11, 7, 2, 8/7, 2, 11, 4
Kendall's	11, 7, 8, 2/7, 2, 11, 8	11, 7, 8, 2/7, 2, 8, 11	11, 7, 2, 8/7, 2, 8, 11
Spearman's	11, 7, 8, 2/7, 2, 11, 8	11, 7, 8, 2/7, 2, 8, 11	11, 7, 2, 8/7, 2, 8, 11
ECR	11, 2, 7, 8/2, 7, 11, 8	–	–
CRR	11, 2, 7, 8/2, 7, 11, 8	–	–
FFTBM-SM	11, 2, 3, 7/2, 11, 7, 3	–	–

can be concluded that from a physics perspective, the FFTBM-SM is a useful prescreening tool for the quantitative evaluation of input uncertain parameters' influence.

In this way, the presented UA in Sec. III.C was supported by information from the sensitivity study in Sec. III.B. It was found useful to perform a sensitivity study before UA despite the fact that it required additional code runs. This is in line with Ref. [29], which recommended the use of sensitivity calculations to ensure the goodness of the analysis. This practice is also in line with the original PTS study, in which sensitivity studies with OAT parameter variation were done too.[1]

From the summary of PTS studies in Ref. [1], it can be seen that break flow, break location, ACC injection temperature, HPSI and LPSI, and HPSI flow control temperature have a significant effect on downcomer conditions. The HPSI flow rate and ACC injection rate have an insignificant impact on downcomer conditions. This qualitative result greatly supports the findings of the quantitative evaluation of input uncertain parameters' influence using FFTBM-SM. (Note that in this study, the break location was fixed.)

III.E.3 Comparison of Sensitivity Study and Sensitivity Analysis Results

The sensitivity analysis presented in Sec. III.D using code runs performed for UA can be done after UA (strictly speaking after the uncertainty code runs are completed). The sensitivity analysis using code runs for UA was used to independently assess the quantitative result obtained by FFTBM-SM. Some care should be taken for ECR and CRR, as the results suggested that a limited sample size led to inconsistencies between the classical CR calculated from the original and rank-

transformed data, which affected the ranking in two out of six cases.

A comparison of the results (see Table III) showed that the most influential parameters identified by the sensitivity study (using qualitative visual observations and quantitative assessment by FFTBM-SM) and the sensitivity analysis generally agreed. The most notable difference was that for FOM2 and FOM3, the decay heat (parameter 3) was ranked among the four highest-ranked parameters, which was not the case for the sensitivity analysis performed by SUSA. When looking at Figs. 8 and 11, decay heat was more influential until 2000s, while OAT suggested after 2000s. According to Ref. [20], OAT designs cannot effectively explore a multidimensional space and OAT approaches are only valid in the case of a linear model.

Here it should be noted that the Spearman's sensitivity measure also lies on a hypothesis of linearity or monotony of the outputs with respect to the inputs (measured by R^2), which is not necessarily satisfied. As can be seen from Fig. 12, for FOM1, a moderate linear relationship was obtained, while for FOM2 and FOM3, moderately strong to fairly strong linear relationships were obtained in the case of the Pearson's and Spearman's correlation types. For the Blomkvist's and Kendall's correlation types, R^2 most of the time was below 0.5, suggesting that the regression model was not very strong.

In Ref. [30], it is stated that the sensitivity analysis is only possible using the probabilistic method and that the results have been demonstrated to be consistent in ranking parameters as influential. This study, using 14 different global sensitivity indices, supported these findings. A paper from 2024[10] also stated that the sensitivity analysis is an essential part of UA, and in that sense, is performed before and after the UA. According to Ref. [10], an a priori sensitivity analysis (i.e., before the UA) is needed to select the input and model parameters that contribute the most to the uncertainty of the safety outputs, and an a posteriori sensitivity analysis can be obtained as a byproduct of the UA and can be used to compare their results with those of the a priori sensitivity analysis.

This study demonstrated an approach for a priori sensitivity study, while in sensitivity analysis, several sensitivity indices were calculated (see the results in Table III) to compare the four highest-ranked influential parameters quantified by FFTBM-SM and the sensitivity indices. The results of this comparison suggest that the sensitivity study using visual observations of sensitivity calculations, complemented with quantitative assessment by FFTBM-SM for OAT input uncertain parameters' variation, can provide useful information for the selection of uncertain input parameters to be used in the UA. It was shown that with a relatively small number of code runs, the influence of the input uncertain parameters can be judged.

The validation activities for the FFTBM-SM confirmed the conclusion from Ref. [13] (for the results obtained in BEMUSE phase II[9]) that FFTBM-SM can provide information on the most influential input parameters and which participant (code and input deck used) is the most sensitive to variations. The conclusions in Ref. [13] for the BEMUSE Phase II agreed well with the conclusions summarized in the final BEMUSE report.[30]

The presented sensitivity analysis in Sec. III.D used most of the sensitivity coefficients used by participants in the BEMUSE programme,[29] which were the Pearson's and Spearman's correlation coefficients, standardized rank regression coefficients, Pearson's and Spearman's partial correlation coefficients, and Sobol indices (not available in SUSA for time-dependent sensitivity analysis). The sensitivity analysis results in Ref. [29] showed that several parameters were ranked as influential by the majority of the 12 participants. For the selected hot-leg LOCA, the results suggested that quantitative evaluation by FFTBM-SM can provide useful information on influential input uncertain parameters.

As can be seen from Table III, for all FOMs, three out of four influential parameters were judged to be the same as those obtained by other sensitivity measures. The results of the quantitative evaluation of input parameters' influence using FFTBM-SM were also supported by PTS studies in Ref. [1], as discussed previously. This is especially important because the sensitivity coefficients listed in Ref. [29] can be obtained after UA, and therefore cannot be used in the selection process of input uncertain parameters.

In the future, it may be interesting to further validate FFTBM-SM for the quantitative evaluation of parameters' influence with the Morris screening method,[12] which is based on derivatives but is classified as a global method because it samples incremental ratios at multiple locations in the input space.[20] It requires a relatively small number of code runs (e.g., for 15 input uncertain parameters, between 80 to 160 code runs would be needed).

IV. CONCLUSIONS

This study investigated the UA and sensitivity analysis of a hot-leg LOCA in a two-loop PWR using RELAP5 version 3.3lj. The analysis used 208 code

simulations to evaluate the impact of 15 input uncertain parameters on key FOMs. The FFTBM-SM methodology was used for quantitative sensitivity assessment, identifying the HPSI temperature, break flow, and initial primary pressure as the most influential parameters.

In the UA, the minimum and maximum values for each FOM were determined over time, representing the lower and upper uncertainty envelopes. The sensitivity analysis utilized 208 sampled runs from the UA to compute the correlation-based sensitivity indices, including the Pearson's ordinary correlation, Blomqvist's medial correlation, Kendall's rank correlation, and Spearman's rank correlation. For each of these correlation types, PCCs, SRCs, and R^2 were calculated. Additionally, classical CRs were calculated from both the original and rank-transformed data.

The results showed that all the methods used, both in the sensitivity study and the global sensitivity analysis, consistently identified the most influential parameters. While slight differences in parameter rankings were observed, the overall findings supported the FFTBM-SM methodology as a prescreening tool for the quantitative evaluation of input uncertain parameters' influence.

This study was limited by the relatively small sample size of 208 simulations, which may affect the accuracy of some sensitivity indices, especially those that are variance based, particularly for less influential parameters. Future research should focus on increasing the sample size to improve the accuracy of global sensitivity analyses and further validate the methodology for the quantitative evaluation of input parameters' influence using FFTBM-SM. Additional efforts could also include validation using the Morris screening method. Expanding the methodology's application to other reactor designs and accident scenarios would further demonstrate its versatility.

Nomenclature

AA = average amplitude

d_i = number of bounds of the FOMs (upper and/or lower)

$F(t)$ = signal

$|\mathcal{F}(f_k)|$ = signal amplitude at the frequency f_k

f = frequency

K = number of points

N = number of calculation runs

p = order

R = number of FOMs

T = analysis time window

t = time

Greek

β = confidence level of the statistical tolerance limits

$\Delta F(t)$ = difference signal

$|\mathcal{\Delta F}(f_k)|$ = difference signal amplitude at the frequency f_k

γ = probability content

Subscripts and superscripts

d = duration

i = i'th FOM

k = k'th frequency

m = power of 2

ref = reference

sm = signal mirroring

var = variation

Acknowledgments

The author acknowledges the Slovenian Nuclear Safety Administration (SNSA) for the arrangement between the U.S. Nuclear Regulatory Commission and SNSA for the exchange of technical information and cooperation. For language improvement of text, ChatGPT-4 version 2025.01.15 was used.

Funding

This work was supported by the Slovenian Research Agency under grant L2-4432, under the core research program P2-0026, and by the Krško nuclear power plant under contract no. Z-8221390 (NEK no. 3221046).

Disclosure Statement

No potential conflict of interest was reported by the author.

ORCID

Andrej Prošek http://orcid.org/0000-0003-0641-3474

References

1. M. E. KIRK et al., "Technical Basis for Revision of the Pressurized Thermal Shock (PTS) Screening Limit in the PTS Rule (10 CFR §50.61)," NUREG-1806, U.S. Nuclear Regulatory Commission (Aug. 2007).
2. P. KRAL et al., "Public Summary Report of WP2," APAL Grant Agreement No.: 945253, Deliverable No. 2.4, Advanced PTS Analysis for LTO Programme, p. 380 (2023).
3. O. C. GARRIDO, A. PROŠEK, and L. CIZELJ, "Pressurized Thermal Shock Preliminary Analyses of a 2-Loop Pressurized Water Reactor Under Loss-of-Coolant Accident Scenarios," *Proc. 30th Int. Conf. on Nuclear Energy for New Europe (NENE-2021)*, pp. 904.1–904.8, Bled, Slovenia, September 6–9, 2021, Nuclear Society of Slovenia (2021).
4. R. TREWIN et al., "Evaluation of Uncertainties in Thermal-Hydraulic Analyses of PTS for the APAL European Project," *Proc. 20th Int. Topl. Mtg. on Nuclear Reactor Thermal-Hydraulics* (*NURETH-20*), pp. 5791–5805, Washington, D.C. August 2023.
5. D. E. BESSETTE et al., "Thermal-Hydraulic Evaluation of Pressurized Thermal Shock," NUREG-1809, U.S. Nuclear Regulatory Commission (2005).
6. C. D. FLETCHER, D. A. PRELEWICZ, and W. C. ARCIERI, "RELAP5/MOD3.2.2y Assessment for Pressurized Thermal Shock Applications," NUREG/CR-6857, U.S. Nuclear Regulatory Commission (2004).
7. R. TREWIN, P. KRAL, and T. NIKL, "Best-Estimate-Plus-Uncertainty Analyses of PTS Using a Mixing-Analysis Program for the APAL European Project," *Proc. 20th Int. Topl. Mtg. on Nuclear Reactor Thermal-Hydraulics (NURETH-20)*, pp. 764–778, Washington, D.C., August 2023.
8. A. PROŠEK and A. VOLKANOVSKI, "RELAP5/MOD3.3 Analyses for Prevention Strategy of Extended Station Blackout," *J. Nucl. Eng. Radiat. Sci.*, **1**, *4*, 041016 (2015); https://doi.org/10.1115/1.4030834.
9. A. DE CRECY et al., "Uncertainty and Sensitivity Analysis of the LOFT L2-5 Test: Results of the BEMUSE Programme," *Nucl. Eng. Des.*, **238**, 3561 (2008); https://doi.org/10.1016/j.nucengdes.2008.06.004.
10. J. FREIXA et al., "Spanish Contribution to the Development and Application of Best Estimate Plus Uncertainty Methodologies: Past, Present and Future," *Nucl. Eng. Des.*, **417**, 112837, pp. 1–22 (2024); https://doi.org/10.1016/j.nucengdes.2023.112837.
11. L. TIBORCZ and S. BECK, "Uncertainty and Sensitivity Analysis of a Postulated Severe Accident in a Generic German PWR with the System Code AC2," *Nucl. Eng. Des.*, **431**, 113670, pp. 1–18 (2025); https://doi.org/10.1016/j.nucengdes.2024.113670.
12. C. WANG, M. PENG, and G. XIA, "Sensitivity Analysis Based on Morris Method of Passive System Performance Under Ocean Conditions," *Ann. Nucl. Energy*, **137**, 107067 (2020); https://doi.org/10.1016/j.anucene.2019.107067.
13. A. PROŠEK and M. LESKOVAR, "Use of FFTBM by Signal Mirroring for Sensitivity Study," *Ann. Nucl. Energy*, **76**, 253 (2015); https://doi.org/10.1016/j.anucene.2014.09.051.
14. E. ZUGAZAGOITIA et al., "Uncertainty and Sensitivity Analysis of a PWR LOCA Sequence Using Parametric and Non-parametric Methods," *Reliab. Eng. Syst. Saf.*, **193**, 106607 (2020); https://doi.org/10.1016/j.ress.2019.106607.
15. "RELAP5/MOD3.3 CODE MANUAL," NUREG/CR-5535/Rev P5, U.S. Nuclear Regulatory Commission (Feb. 2019, revised May 12, 2022).
16. A. PROŠEK and M. MATKOVIČ, "RELAP5/MOD3.3 Analysis of the Loss of External Power Event with Safety Injection Actuation," *Sci. Technol. Nucl. Ins.*, **2018**, 6964946 (2018).
17. "Symbolic Nuclear Analysis Package (SNAP), User's Manual," Version 3.1.9, Applied Programming Technology, Inc. (Aug. 2, 2021).
18. W. AMBROSINI, R. BOVALINI, and F. D'AURIA, "Evaluation of Accuracy of Thermalhydraulic Code Calculations," *Energia Nucleare*, **7**, 5 (1990).
19. A. PROŠEK, M. LESKOVAR, and B. MAVKO, "Quantitative Assessment with Improved Fast Fourier Transform Based Method by Signal Mirroring," *Nucl. Eng. Des.*, **238**, 2668 (2008); https://doi.org/10.1016/j.nucengdes.2008.04.012.
20. A. SALTELLI et al., "Why So Many Published Sensitivity Analyses Are False: A Systematic Review of Sensitivity Analysis Practices," *Environ. Modell. Software*, **114**, 29 (2019); https://doi.org/10.1016/j.envsoft.2019.01.012.
21. A. PROŠEK, F. D'AURIA, and B. MAVKO, "Review of Quantitative Accuracy Assessments with Fast Fourier Transform Based Method (FFTBM)," *Nucl. Eng. Des.*, **217**, 179 (2002); https://doi.org/10.1016/S0029-5493(02)00152-8.
22. M. KLOOS and B. NADINE, "SUSA, Software for Uncertainty and Sensitivity Analyses, Classical Methods," GRS-631, Gesellschaft für Anlagen- und Reaktorsicherheit, gGmbH (2021).
23. A. PROŠEK and B. MAVKO, "The State-of-the-Art Theory and Applications of Best-Estimate Plus Uncertainty Methods," *Nucl. Technol.*, **158**, *1*, 69 (2007); https://doi.org/10.13182/NT07-1.
24. M. KLOOS, "SUSA Version 4.2, User's Guide and Tutorial, Software for Uncertainty and Sensitivity Analyses (SUSA)," Version 4.2.6, Gesellschaft für Anlagen- und Reaktorsicherheit, gGmbH (Oct. 2020, part of the Help menu in SUSA).

25. "BEMUSE Phase II Report—Re-Analysis of the ISP-13 Exercise, Post Test Analysis of the LOFT L2-5 Test Calculation," NEA/CSNI/R(2006)2, p. 19, Organisation for Economic Co-operation and Development/Nuclear Energy Agency (2005).

26. A. PROŠEK and B. MAVKO, "Quantitative Assessment of Time Trends: Influence of Time Window Selection," *Proc. 5th Int. Conf. Nuclear Option in Countries with Small and Medium Electricity Grids*, Dubrovnik, Croatia, May 16–20, 2004, Croatian Nuclear Society (2004).

27. N. W. PORTER, "Wilks' Formula Applied to Computational Tools: A Practical Discussion and Verification," *Ann. Nucl. Energy*, **133**, 129 (2019); https://doi.org/10.1016/j.anucene.2019.05.012.

28. TECHNICAL PROGRAM GROUP, B. E. BOYACK et al., "Quantifying Reactor Safety Margin Parts 1 to 6," *Nucl. Eng. Des.*, **119**, *1*, 1 (1990); https://doi.org/10.1016/0029-5493(90)90071-5.

29. M. PEREZ et al., "Uncertainty and Sensitivity Analysis of a LBLOCA in a PWR Nuclear Power Plant: Results of the Phase V of the BEMUSE Programme," *Nucl. Eng. Des.*, **241**, 4206 (2011); https://doi.org/10.1016/j.nucengdes.2011.08.019.

30. "BEMUSE Phase VI Report—Status Report on the Area, Classification of the Methods, Conclusions and Recommendations," Organisation for Economic Co-operation and Development/Nuclear Energy Agency (2008).